Check for updates

RESEARCH ARTICLE

REVISED **Mutation profiling of anaplastic ependymoma grade III by Ion Proton next generation DNA sequencing [version 2; peer review: 2 approved]**

Ejaz Butt[1,2], Sabra Alyami[3], Tahani Nageeti[4], Muhammad Saeed[5], Khalid AlQuthami 🆔[6], Abdellatif Bouazzaoui[7], Mohammad Athar[7], Zainularifeen Abduljaleel[7], Faisal Al-Allaf[7], Mohiuddin Taher 🆔[7]

[1]Histopathology Division, Al-Noor Specialty Hospital, Makkah, Makkah, Saudi Arabia
[2]Histopathology Department, Amna Inayat Medical College, Sheikhupura, Punjab, Pakistan
[3]Department of Medical Genetics, Umm-Al-Qura University, Makkah, Makkah, Saudi Arabia
[4]Department of Radiation Oncology, King Abdullah Medical City, Makkah, Makkah, Saudi Arabia
[5]Faculty of Medicine, Umm-Al-Qura University and Al-Noor Specialty Hospital, Makkah, Makkah, Saudi Arabia
[6]Department of Laboratory Medicine and Blood Bank, Al-Noor Specialty Hospital, Makkah, Makkah, Saudi Arabia
[7]Department of Medical Genetics and Science and Technology Unit, Umm-Al-Qura University, Makkah, Makkah, Saudi Arabia

Abstract

Background: Ependymomas are glial tumors derived from differentiated ependymal cells. In contrast to other types of brain tumors, histological grading is not a good prognostic marker for these tumors. In order to determine genomic changes in an anaplastic ependymoma, we analyzed its mutation patterns by next generation sequencing (NGS).
Methods: Tumor DNA was sequenced using an Ion PI v3 chip on Ion Proton instrument and the data were analyzed by Ion Reporter 5.6.
Results: NGS analysis identified 19 variants, of which four were previously reported missense variants; c.395G>A in *IDH1*, c.1173A>G in *PIK3CA*, c.1416A>T in *KDR* and c.215C>G in *TP53*. The frequencies of the three missense mutations (*PIK3CA* c.1173A>G, *KDR* c.1416A>T, *TP53*, c.215C>G) were high, suggesting that these are germline variants, whereas the *IDH1* variant frequency was low (4.81%). However, based on its FATHMM score of 0.94, only the *IDH1* variant is pathogenic; other variants *TP53*, *PIK3CA* and *KDR* had FATHMM scores of 0.22, 0.56 and 0.07, respectively. Eight synonymous mutations were found in *FGFR3*, *PDGFRA*, *EGFR*, *RET*, *HRAS*, *FLT3*, *APC* and *SMAD4* genes. The mutation in *FLT3* p.(Val592Val) was the only novel variant found. Additionally, two known intronic variants in *KDR* were found and intronic variants were also found in *ERBB4* and *PIK3CA*. A known splice site mutation at an acceptor site in *FLT3*, a 3'-UTR variant in the *CSF1R* gene and a 5'_UTR variant in the *SMARCB1* gene were also identified. The p-values were below 0.00001 for all variants and the average coverage for all variants was around 2000x.
Conclusions: In this grade III ependymoma, one novel synonymous mutation and one deleterious missense mutation is reported. Many of the

Open Peer Review

Reviewer Status ✔✔

	Invited Reviewers	
	1	**2**
version 2 (revision) 22 Jun 2020	✔ report	
	⬆	
version 1 02 May 2019	❓ report	✔ report

1 **Luni Emdad**, Virginia Commonwealth University, Richmond, USA

2 **Firoz Ahmad**, SRL Ltd, Mumbai, India

Any reports and responses or comments on the article can be found at the end of the article.

variants reported here have not been detected in ependymal tumors by NGS analysis previously and we therefore report these variants in brain tissue for the first time.

Keywords

Ependymoma, Palisading necrosis, Perivascular psuedorossettes, Ion Proton, Next Generation DNA sequencing, Glioma, pediatric brain tumors, Anaplastic Ependymoma

Corresponding author: Mohiuddin Taher (virginia23223@yahoo.com)

Author roles: Butt E: Investigation, Visualization; **Alyami S**: Data Curation, Writing – Original Draft Preparation; **Nageeti T**: Data Curation, Project Administration, Resources; **Saeed M**: Formal Analysis, Investigation, Visualization, Writing – Original Draft Preparation; **AlQuthami K**: Data Curation, Resources; **Bouazzaoui A**: Methodology; **Athar M**: Data Curation, Resources; **Abduljaleel Z**: Software; **Al-Allaf F**: Project Administration, Supervision; **Taher M**: Conceptualization, Funding Acquisition, Supervision, Writing – Review & Editing

The first author's name was printed as Muhammad Butt in the first published version of the manuscript. His first name is Ejaz, and the last name is Butt. I have corrected this in the revised manuscript.

The NGS analysis reported here is for a single case, as suggested by both referees, we have modified the statement for specimen collection in the revised manuscript in the 'Methods' section. As suggested by the 2nd reviewer, we have indicated tumor tissue content of the FFPE block used in this investigation in the 'Methods' section.

The 1st referee had asked to add additional correlation analysis by analyzing TCGA or other bioinformatics-based data for the signature molecules in the context of grade III ependymoma. As suggested, we have searched various databases including 'The Cancer Genome Atlas' (TCGA), in cBioportal database, ICGC data portal, in the NCI's Genomic Data Commons (GDC) portal, and in NCI supported Clinical Trials portal, and a relevant section of this summary is included in the revised manuscript in the 'Discussion' section. The tumor type we described in this study is a rare tumor, and specifically, in many databases, it is not listed separately except in the 'Integrative onco-genomics' database (https://www.intogen.org). Both referees had suggested commenting on the FLT3 novel synonymous variant, we have added this in the 'Discussion' section. Also, in the 'response to referees' files, we have explained for their comments in detail. In the modification process, we have added 7 new references in the revised-manuscript, and citations are rearranged. As suggested by the reviewer-1 the corrections are made in Figure 2, and a new with figure legend is added in the revised manuscript.

Any further responses from the reviewers can be found at the end of the article

Introduction

Ependymal cells are macroglial cells which line the ventricles, the central canal of the spinal cord and form the blood-cerebrospinal fluid barrier, being involved in producing the cerebrospinal fluid[1,2]. These tumors account for only 4–8% of gliomas and, after astrocytomas and oligodendrogliomas, ependymomas are the least common[3]. Nearly one-third of brain tumors in patients younger than three years old are ependymomas and constitute around 5%–9% of all neuroepithelial malignancies[1,4]. These tumors are also found in the choroid plexus and may occur at any age, from one month to 81 years and without any gender preference[5]. In pediatric cases, the location of the tumor is intracranial, while adult ependymal tumors can have either an intracranial or a spinal localization[6,7]. The prognosis is better in older children as compared to young infants but nonetheless, in children with intracranial ependymomas, event-free survival after five years is less than 50%[8]. In adults, about 50% to 60% intracranial ependymomas are supratentorial; however, pediatric supratentorial ependymomas account for 25% to 35% of all ependymomas[5,9]. Adults present better prognosis with a 5-year survival of around 90%, while in the pediatric population it is around 60%. The five-year survival rate for supratentorial, infratentorial, and spinal cord ependymomas is 62%, 85%, and 97%, respectively, and for grade I, II, and III spinal cord ependymomas the five-year overall survival rate is 92%, 97% and 58%, respectively[10–12].

Ependymoma tumors are well circumscribed, soft, tan-red masses and may be associated with hemorrhage. Their microscopic appearance shows hypercellularity and distinct infiltrative margins with surrounding parenchyma, consisting of monomorphic cells with nuclear atypia and brisk mitotic activity. They may also have intramural or glomeruliod vascular proliferation, pseudopalisading necrosis, perivascular pseudo rosettes (5–10% cases), calcifications and hyalinized vessels[1]. Other diagnostic hallmarks include areas of fibrillary and regressive changes such as myxoid degeneration, palisading necrotic areas and the formation of true rosettes, composed of columnar cells arranged around a central lumen[1,6]. Immunologically, they are positive for epithelial membrane antigen (EMA), glial fibrillary acidic protein (GFAP) and S-100. According to the 2016 updated World Health Organization (WHO) classification of brain tumors, ependymomas are divided into 4 types on the basis of histologic appearance: (1) grade I subependymomas, (2) grade I myxopapillary ependymomas, (3) grade II ependymomas, (4) grade II or III *RELA* fusion-positive ependymomas and grade III anaplastic ependymomas[13,14].

Previous studies have shown the use of comparative genomic hybridization (CGH) arrays to distinguish intracranial ependymomas from spinal ependymomas[15]. In contrast to other types of brain tumors, histological grading is not a good prognostic marker for outcome for ependymomas[16,17]. Several gene expression studies have been helpful in differentiating between intracranial and extra cranial ependymomas, but have not had clinical significance in directing therapy and their role in tumor origin and prognosis is not clear[18,19]. Studies using cDNA microarrays have shown that gene expression patterns in ependymomas correlate with tumor location, grade and patient age[20]. Cytogenetic studies have shown that chromosomal abnormalities are relatively common in ependymomas[21]. Loss of 22q has been the commonest abnormality found in ependymoma and, in some other tumors, gain of 1q or loss of 6q was observed[21,22].

To date, there is a lack of information regarding the mutational signatures which distinguish the various subgroups of ependymomas. Another ependymoma cohort study found very few mutations and gene amplifications but a high expression of multi-drug resistance, DNA repair and synthesis enzymes[23]. Intracranial ependymomas differ from spinal ependymomas in the expression of these proteins, and protein expression is also dependent on the ependymoma grade[23]. For both intracranial and spinal ependymomas, very few mutations were reported by using whole exome sequencing[24]. In another study, profiling of NGS mutations was carried out for one case of grade II ependymoma using a GlioSeq panel, which contains a total of 30 genes[25]. In order to determine the mutational patterns of grade III anaplastic ependymoma, we have sequenced DNA from this ependymoma tumor using the Ion Proton system for next generation DNA sequencing with the Ion Torrent's AmpliSeq cancer HotSpot panel. This panel contains 50 genes, only 15 of which also appear in the GlioSeq panel used in previous research. These data provided an evaluation of mutational signatures of this anaplastic ependymoma which differs

from the previous two studies, but confirms their conclusions about finding very few mutations in cancer driver genes, helping to direct diagnosis and therapy for ependymomal tumors.

Methods
Ethical statement
This study was performed in accordance with the principles of the Declaration of Helsinki. This study was approved by the Institutional Review Board (IRB) bioethics committee of King Abdullah Medical City (KAMC), Makkah, Kingdom of Saudi Arabia (IRB number 14-140). A written informed consent was obtained from the parent of this patient before starting the study.

Clinical specimen
The single patient's tumor tissue (FFPE sections in PCR tubes) used in this NGS analysis was obtained from the histopathology laboratory of Al-Noor Specialty Hospital Makkah, after tumor excision and left frontal craniotomy in the neurosurgery department. The tumor content of the FFPE tissues was around 70–80%. The tumor was classified based upon similarity to the constituent cells of the central nervous system, such as astrocytes, oligodendrocytes and ependymal, glial cells, mitosis and cell cycle-specific antigens, used as markers to evaluate proliferation activity and biological behavior (the WHO grading system)[13]. The final diagnosis was made following radiological, histopathological and immunological examinations.

Radiology and histopathological analysis
A CT scan of the brain was performed by a multi-slice CT (MSCT), using a 64-detector-row scanner. The use of computed tomography (CT) allowed visualization of detailed images of the soft tissues in the body in 3D as well as in multiplanar reconstructions. Images were acquired with 5mm slice thickness throughout on a GE Medical Systems, light speed VCT, 64-slice multidetector CT (MDCT). High quality images were processed at low dose performance on Volara™ digital DAS (Data Acquisition System).

The excised tumor was fixed in 4% buffered formaldehyde, routinely processed and paraffin embedded. Four-micrometer-thick sections were prepared on clear ground glass microscope slides with ground edges and routinely stained using Dako Reagent Management System (DakoRMS) with hematoxylin and eosin (H and E) on a Dako Coverstainer (Agilent). For immunohistochemistry, sections were collected on Citoglas adhesion microscope slides (Citotest). Mouse monoclonal beta-catenin (14) (Sigma-Aldrich, cat. no. 224M-1), mouse monoclonal EMA (E29) (Sigma-Aldrich, cat. no. 247M-9), rabbit monoclonal EGFR (SP84) (Cell Marque, cat. no. 414R-16-ASR), mouse monoclonal Vimentin (vim 3B4) (Ventana-Roche, cat. no. 760-2512), GFAP EP672Y rabbit monoclonal (Ventana-Roche, cat. no. 760-4345) and E-cadherin (36) mouse monoclonal (Ventana-Roche, cat. no. 790-4497) and mouse monoclonal anti-Ki-67 (Leica Biosystems, cat. no. KI67-MM1-L-CE) antibodies were used for immunohistochemistry. Briefly, the tissue sections were deparaffinized with EZ Prep (Ventana, cat. no. 950-102) at 60°C for 1 hr. Immunohistochemistry was performed with the Ventana

BenchMark XT automated stainer (Ventana, Tucson, AZ). After inactivation of the endogenous peroxidase using a UV-inhibitor for 4 min at 37°C, the primary antibody was added for 16 min at 37°C, followed by the application of HRP Universal Multimer for 8 min, and detected using the ultraView Universal DAB Detection Kit (cat. no. 760-500) for 38 min. Slides were counterstained with hematoxylin for 8 min and bluing reagent for 4 min before mounting with cover slips. Following staining, images were acquired using NIKON Digital Microscope Camera - DS-Ri1, with image software NIS Elements v.4.0. Appropriate positive controls for all of the studied antibodies were used.

DNA isolation and NGS analysis
DNA isolation was carried out using the QIAamp DNA FFPE Kit (50), Cat. No. 56404. 5-10 Formalin-Fixed Paraffin-Embedded sections of 5 microns were deparaffinized using xylene, treated with ethanol to remove the xylene, and the pellet was dried at 65°C for 5 mins. The pellets were resuspended in ATL buffer then treated with proteinase K. The remaining steps were carried out according to the user manuals. DNA concentration was measured using Nanodrop2000C and 10 ng of DNA was used for NGS analysis. DNA was sequenced using the Ion PI v3 Chip Kit (Cat no. A25771, Thermo Fisher Scientific, USA) with the Ion Proton System (Cat no. 4476610, Thermo Fisher Scientific, USA)[26]. Libraries were prepared using Ion AmpliSeq cancer HotSpot Panel v1 (Cat no. 4471262, Thermo Fisher Scientific, USA) primer pools. The Ion AmpliSeq Library Kit 2.0 (Cat no. 4475345, Thermo Fisher Scientific, USA) and Ion PI Hi-Q OT2 200 Kit (Cat no. A26434, Thermo Fisher Scientific, USA) was used for library and template preparation respectively. Sequencing was carried out using Ion PI Hi-Q Sequencing 200 Kit (Cat no. A26433, Thermo Fisher Scientific, USA) reagents and libraries were tagged with Ion Express Barcode Adapters 1-16, Cat. No. 4471250 (Thermo Fisher Scientific, USA). After sequencing, amplicon sequences were aligned to the human reference genome GRCh37 (hg19) (Accession no. GCA_000001405.1) in the target region of the cancer HotSpot panel using the Torrent Suite Software v.5.0.2 (Thermo Fisher Scientific, USA). Variant call format files (vcf files) were generated by running the Torrent Variant Caller Plugin v5.2. Variant calling and creation of vcf files can also be carried out using non-proprietary software such as SAMtools[27] or VarScan2[28], which also provide coverage analysis. The vcf file data were analyzed using Ion Reporter v5.6 (ThermoFisher Scientific, USA), which calculated allele coverage, allele frequency, allele ratio, variant impact, clinical significance, PolyPhen 2 scores, Phred scored, SIFT scores, Grantham scores and FATHMM scores. This vcf file analysis was also carried out by Advaita Bioinformatics' iVariantGuide. PolyPhen2, SIFT, variant impact and clinical significance can be calculated using non-proprietary software SnpEff[29] and SnpSift[30]. FATHMM scores can also be predicted using fathmm[31] and Grantham scores according to the formula as described in Grantham, 1974[32]. The heat map was generated by the clustering of predicted variant impact scores by Ion Reporter v5.6. The most deleterious score was picked for every gene to generate the heat map; thereafter, hierarchical clustering was conducted. The color codes indicate the following variant impacts using score values 0-8: (0) unknown; (1) synonymous;

(2) missense; (3) non-frameshift block substitution; (4) non-frameshift indel; (5) nonsense; (6) stop-loss; (7) frameshift block substitution or indel; (8) splice variant.

Results
Clinical presentation and radiology
A six-year-old female patient presented with a history of right facial palsy for few months with ataxia and right-sided weakness. The patient had a chronic headache, vomiting and had repeatedly been treated for sinusitis. Unenhanced computed tomography (CT) of the brain was performed (Figure 1, panels A, B and C). A large lesion (5.4 × 7.5cm) was noticed in the left cerebral frontoparietal region. There was an indication of a predominant cystic component and large, eccentric clump of coarse calcification. Additionally, mass effect resulting in midline shift, along with mild scalloping of the internal cortex of the parietal bone, was noted. No hydrocephalic changes or intrinsic hemorrhagic focus were seen (Figure 1).

Histopathological examination revealed sheets of neoplastic cells with round to oval nuclei and abundant granular chromatin. A variable dense fibrillary background and endothelial proliferation was also noted. Hematoxylin and eosin (H&E) staining results are shown in Figure 2 and Figure 3. Panels A and B of Figure 2 show the tumor exhibiting delicate cytoplasmic processes, perivascular rosettes characteristic of ependymoma, focal calcification areas and pseudo palisading necrosis, characterized by a garland-like structure of hypercellular tumor nuclei lining up around irregular foci of tumor necrosis. Panel C shows glomeruloid vascular proliferation and panel D shows extensive palisading necrosis and true rosette formation. The exhibition of a true rosette with a central lumen and the formation of pseudo-palisading necrotic areas is also clear from Figure 3 (panel A). Panel B shows focal areas with numerous tumor giant cells and the presence of brisk mitotic activity, vascular formation and pseudo-palisading necrotic areas. Formation of true rosettes surrounding the microvascular proliferation

within ependymal tumors usually signifies anaplastic transformation, which is characteristic of grade III ependymoma (panels C and D). Immunostaining is shown in Figure 4: (A) Ki-67 stain shows a high proliferation index, (B) vimentin positive, (C) GFAP positive, (D) EMA showing punctate cytoplasmic (perinuclear dot-like positivity) staining which is fairly diagnostic of ependymal tumor cells. Figure 5 shows beta-catenin positive (panels A and B) and E-cadherin positive (panels C and D) immunostaining, with both membranous and true rosette-like structures clearly visible in this staining. EGFR staining was negative (see *Underlying data*)[33].

NGS data analysis variant identification and variant statistics
Alignment to the target regions (CHP2. 20131001.designed) of the reference genome (hg 19) was performed by the Ion Torrent Suite software v.5.0.2. For this tumor, NGS generated 6,252,341 mapped reads using the Ion PI v3 Chip, with more than 90% reads on target. Amplicon and target base read coverages for the sequencing are shown in Table 1. All 207 amplicons were sequenced with Ion AmpliSeq Cancer HotSpot Panel primer pool. As shown in Table 1, for this sample sequencing the uniformity of amplicon coverage was 95.17%, and the uniformity of base coverage on target was 94.81%. The average reads per amplicon was 34, 179, and the average target base coverage depth was 31,771. 100% of amplicons had at least 500 reads and the percentage of amplicons read end-to-end was 89.37% (Table 1). Initial analysis by the Ion Reporter 5.6 program found that a total of 1652 variants passed all filters. Initial analysis by Advaita's iVariantGuide software showed 100% (1633) of variants passed all filters (see *Extended data*)[33]. The filter flags signify variants which do not meet certain criteria during variant calling. The flags refer to the quality or confidence of the variant call. The parameters of flags were read in from the input vcf file. If a variant passes all filters, it is marked as having passed. Six hundred and fifteen variants were identified using a filter for clinical significance that identifies drug response, likely to be
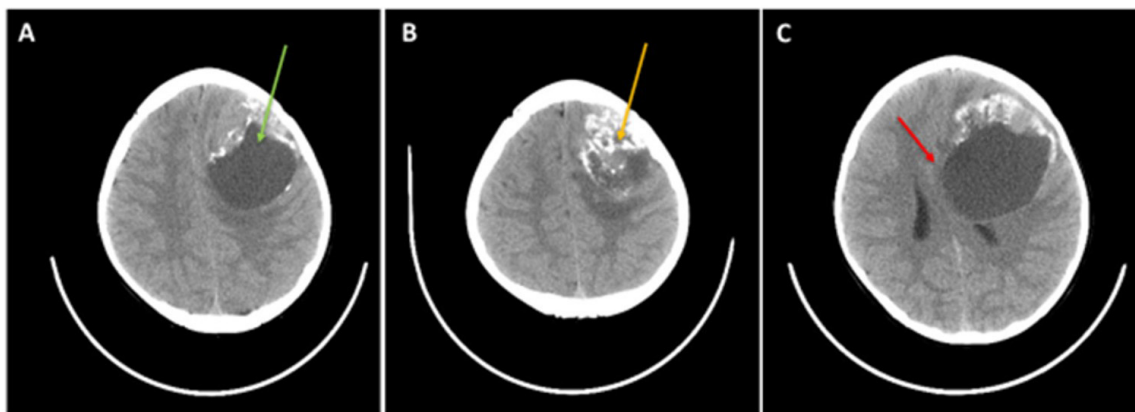
Figure 1. Grade III ependymoma unenhanced computed tomography (CT) of the brain. A large lesion (5.4 × 7.5cm) in the left cerebral frontoparietal location with predominantly cystic components (panel **A**, green arrow), and a large, eccentric clump of coarse calcification (panel **B**; yellow arrow). Mass effect and mid line shift (panel **C**, red arrow) can also be seen. No hydrocephalic changes or intrinsic active hemorrhagic focus were observed.
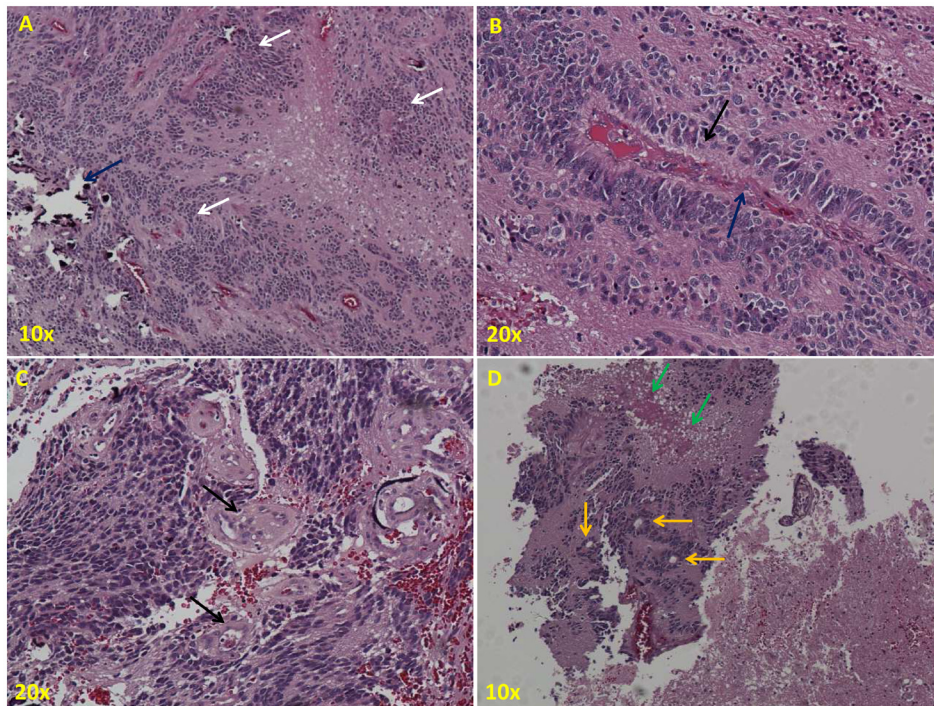
Figure 2. Hematoxylin and eosin (H&E) staining showing anaplastic ependymoma features. (**A**) Focal calcification areas (blue arrow), and perivascular pseudo-rosettes (white arrow). (**B**) Pseudo palisading necrosis, characterized by a garland-like structure of hypercellular tumor nuclei (black arrow) lining up around irregular foci of tumor necrosis (blue arrow). (**C**) The cellular tumor exhibiting glomeruloid vascular proliferation (black arrows). (**D**) Extensive palisading necrosis (green arrows) and true rosettes (yellow arrows).
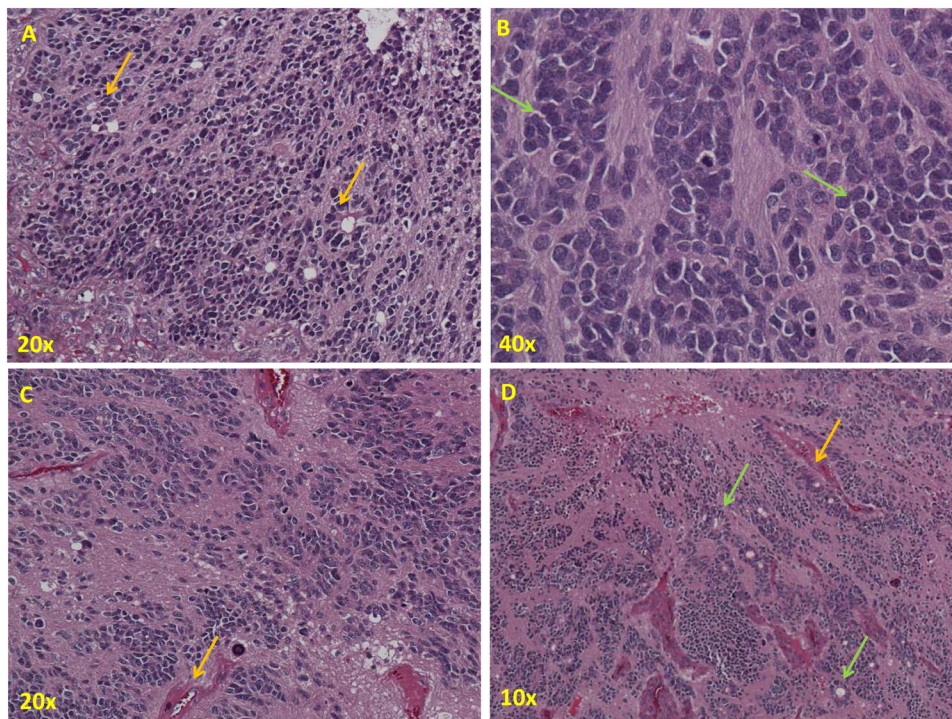
Figure 3. Hematoxylin and eosin (H&E) staining showing anaplastic ependymoma features. (**A**) Pseudo palisading necrotic areas, exhibiting true rosettes with central lumen (yellow arrow). (**B**) Focal areas with numerous tumor giant cells and the presence of a brisk mitotic activity (green arrows). (**C**) Tumor with vascular formation (yellow arrows) and pseudo palisading necrotic areas. (**D**) Formation of true rosettes (green arrows) surrounding the microvascular proliferation within ependymal tumors, usually signifies anaplastic transformation which is characteristic of ependymomas.
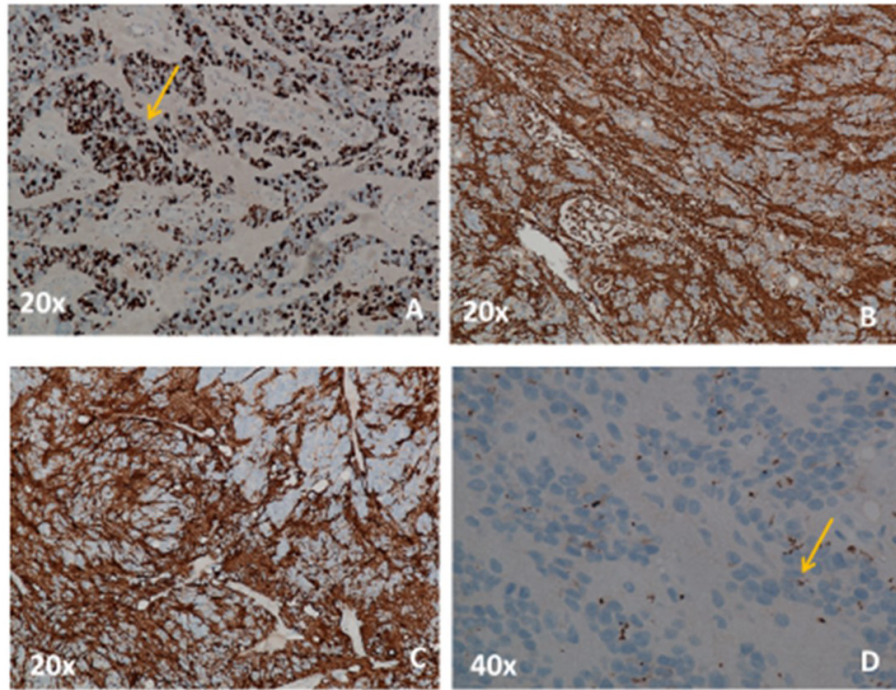
Figure 4. Photomicrographs of Ki-67, vimentin, GFAP, and EMA immunostaining of the ependymal tumor. (**A**) Ki-67 immunostaining indicates a high proliferation index in the tumor (70%). (**B**) Vimentin stain is positive. (**C**) GFAP stain is positive. (**D**) EMA stain is positive and shows punctate cytoplasmic (perinuclear dot-like) staining, fairly diagnostic of the ependymal nature of the tumor cells.
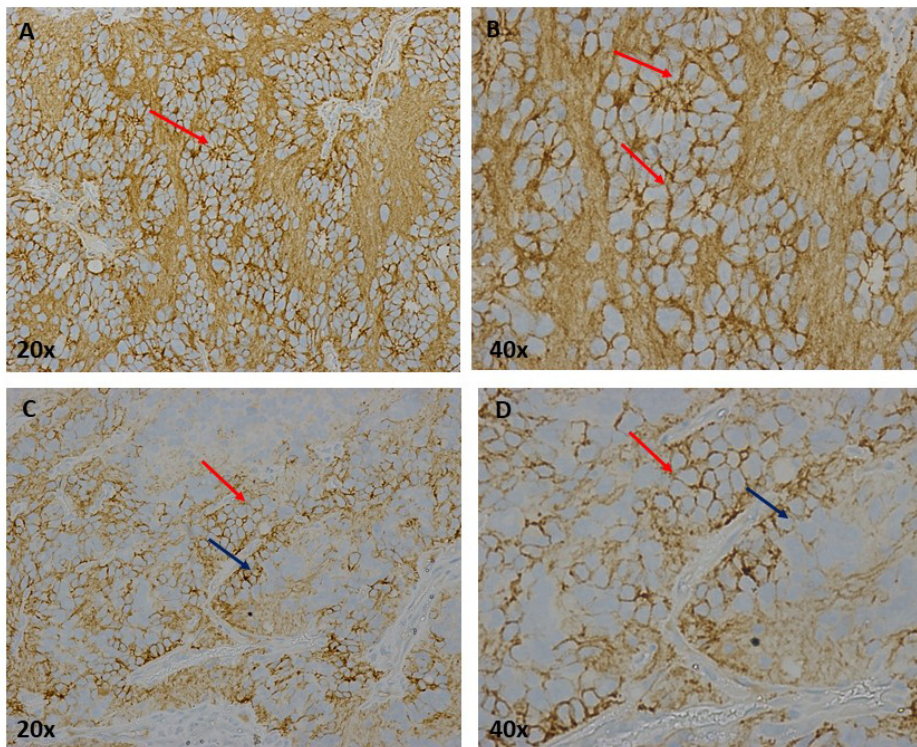
Figure 5. Photomicrographs of beta-Catenin and E-Cadherin immunostaining of the ependymal tumor. Immunostaining is strongly positive for beta-Catenin (panel **A** 20x, panel **B** 40x) and true rosettes (red arrows) and palisading cells (blue arrow) are clearly visible. E-Cadherin stain is also positive in this tumor. Red and blue arrows indicate tumor cells arranged in true rossettes and formation of palisading structures, respectively (panel **C** 20x, panel **D** 40x).

Table 1. Coverage analysis of the tumor DNA sequencing on Ion Proton.

Amplicon Read Coverage		Target Base Coverage	
Number of amplicons	207	Bases in target regions	22,027
Percent assigned amplicon reads	97.53%	Percent base reads on target	89.69%
Average reads per amplicon	34, 179	Average base coverage depth	31,771
Uniformity of amplicon coverage	95.17%	Uniformity of base coverage	94.81%
Amplicons with at least 1 read	100%	Target base coverage at 1x	100%
Amplicons with at least 20 reads	100%	Target base coverage at 20x	100%
Amplicons with at least 100 reads	100%	Target base coverage at 100x	100%
Amplicons with at least 500 reads	100%	Target base coverage at 500x	100%
Amplicons with no strand bias	97.58%	Target bases with no strand bias	96.35%
Amplicons reading end-to-end	89.37%	Percent end-to-end reads	86.80%

pathogenic and pathogenic variants. The distribution of these variants, based on chromosomal position, region within the gene, variant class, functional class, variant impact and clinical significance, are shown in doughnut charts A – F (Figure 6). As shown in doughnut chart A, chromosome 17 has the highest number of variants (26%) and chromosome 8 has lowest number of variants (0.8%). 98.7% of variants are exonic and, according to variant class distribution, 73.8% are SNPs, 70.2% are missense variants, 25.4% are high impact variants and 46.8% are pathogenic. We have considered true mutations to be those with a Phred score above 20 and significant mutations called by Ion Reporter software were those with a p-value below 0.05.

A summary of the all missense mutations found in the grade III tumor is shown in Table 2. In this tumor, NGS data analysis identified 19 variants, of which four were missense mutations, eight were synonymous mutations and seven were intronic variants. Known missense mutation c.395G>A; p.(Arg132His) in exon 4 of the *IDH1* gene, c.1173A>G; p.(Ile391Met) in exon 7 of the *PIK3CA* gene, c.1416A>T; p.(Gln472His) in exon 11 of the *KDR* gene and c.215C>G; p.(Pro72Arg) in exon 4 of the *TP53* gene were found in this tumor. The frequency, allele coverage, allele ratio, p-value and Phred score for these mutations is shown in Table 3. The p-values and Phred scores were significant for all of these mutations. The frequencies of the three missense mutations, namely *PIK3CA* c.1173A>G, *KDR* c.1416A>T and *TP53* c.215C>G, were high, suggesting that these are germ line variants, whereas the *IDH1* variant frequency was low (4.81%). As shown in Table 2, eight synonymous mutations were found in this tumor, in exon 14 of *FGFR3* p.(Thr651Thr), exon 12 of *PDGFRA* p.(Pro566Pro), exon 20 of *EGFR* p.(Gln787Gln), exon 13 of *RET* p.(Leu769Leu), exon 2 of *HRAS* p.(His27His), exon 14 of *FLT3* p.(Val592Val), exon 16 of *APC* p.(Thr1493Thr) and exon 9 of *SMAD4* p.(Phe362Phe). The synonymous mutation in *FLT3* (c.1776T>C; p.(Val592Val) detected in this tumor was a novel variant, while the other variants were previously reported. Additionally, two known intronic variants were identified in *KDR* (c.798+54G>A and c.2615-36A>CA) (Table 2). A known splice site mutation (c.1310-3T>C) at an

acceptor site in *FLT3* (rs2491231) and a single nucleotide variant in the 3'-UTR of the *CSF1R* gene (rs2066934) were also identified. Additionally, in *SMARCB1* a 5'-UTR variant, and an intronic variant in *ERBB4* and *PIK3CA* respectively were found. In Figure 7, the heat map of the variant impact for each gene is presented. The color gradation from green to red indicates unknown, synonymous, missense, nonsense, and splice variants, based upon their SIFT, PolyPhen2 and Grantham scores. Only variants in four genes had a positive PolyPhen2 score (variants in *TP53, PIK3CA, IDH1* and *KDR* genes had a PolyPhen2 score of 0.083, 0.011, 0127 and 0.003, respectively). However, FATHMM scores for the prediction of the functional consequences of a variant suggest that only the *IDH1* variant is pathogenic, with a score of 0.94. As described in the COSMIC data base, FATHMM scores above 0.5 are deleterious, but only scores ≥ 0.7 are classified as pathogenic.

Discussion

Ependymomas are brain tumors that arise throughout the central nervous system, within the supratentorial areas, the posterior fossa and the spinal cord. Histologic low-grade (WHO grade I) tumors, such as subependymomas and myxopapillary ependymomas, are usually slow progressing variants of ependymomas. In contrast, grade III ependymomas display anaplastic features like hypercellularity, high mitosis, proliferation of endothelial cells and palisading necrosis[34]. Histopathological evaluation of ependymoma tissue reveals pseudo-rosette formation, high mitotic activity, vascular proliferation and necrosis, EMA staining with perinuclear dot-like structures and with diffuse GFAP immunoreactivity[35]. Immunological staining with GFAP and vimentin is very helpful for the differential diagnosis of ependymomas from other non-ependymal tumors, such as astrocytic and choroid plexus tumors, and also in differentiating between the various grades of ependymomas[13,14,36]. It has been reported that the GFAP expression correlates with a loss of E-cadherin expression in anaplastic ependymomas, although in this case there was E-cadherin expression[36]. Changes in E-cadherin expression promote tumor invasion and metastasis[37]. Overexpression of EGFR is known to correlate with tumor grades in ependymomas
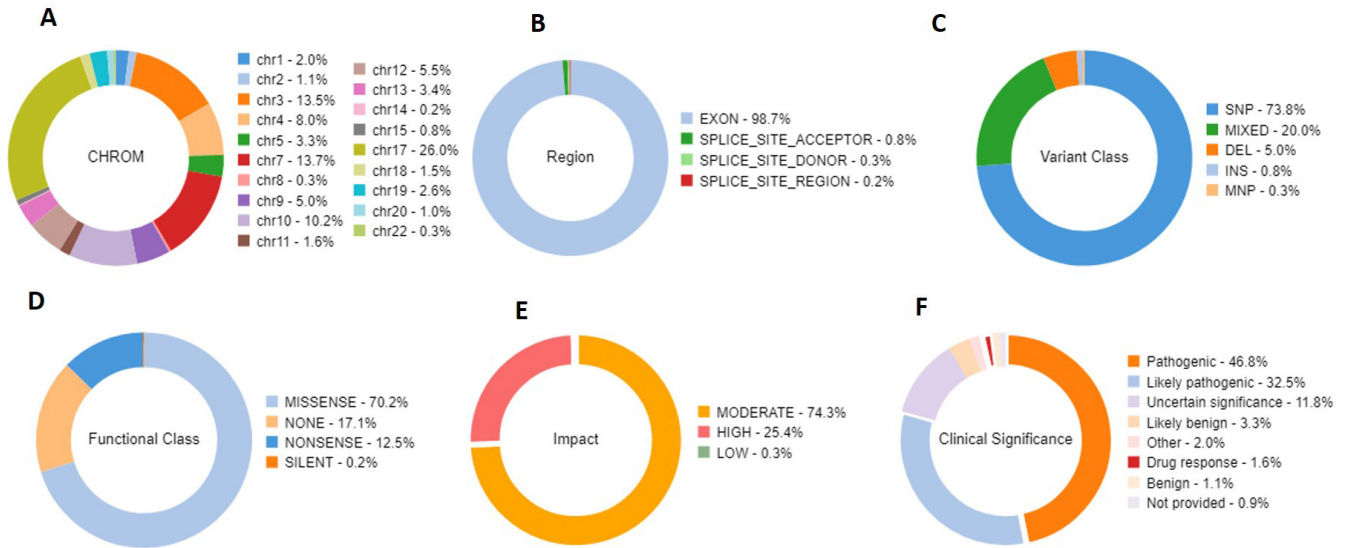
Figure 6. iVariant analysis of variant characteristics. Distribution of variants according to filters, showing characteristics including the relative number of variants located on each chromosome, variant class, substitution type and the functional consequences of each variant, in order to interpret and score the severity and impact of variants and therefore predict the severity of the disease. Doughnut charts in panels shows variants passed for each individual filter for (**A**) Chromosomal distribution, (**B**) Region in the gene, (**C**) Variant class, (**D**) Variant effect on the protein structure, (**E**) Variant impact on the protein function and (**F**) Clinical significance of the variants as annotated on the ClinVar database.

Table 2. Variants found in the grade III ependymoma tumor.

Chromosomal Position	Ref	Observed Allele	% Frequency	Gene	Coding	COSMIC/ dbSNP	AA Change	Exon
chr2:209113112	CG	TG	4.81	IDH1	c.395G>A	COSM28746	p. (Arg132His)	4
chr2:212812097	T	C	100	ERBB4	c.421+58A>G	rs839541	p.?	
chr3:178917005	A	G	47.97	PIK3CA	c.352+40A>G	rs3729674	p.?	
chr3:178927410	A	G	54.25	PIK3CA	c.1173A>G	COSM328028	p. (Ile391Met)	7
chr4:1807894	G	A	100	FGFR3	c.1953G>A	rs7688609	p. (Thr651Thr)	14
chr4:55141050	AGCCCAGA	AGCCCGGA	100.00	PDGFRA	c.1701A>G	rs1873778	p. (Pro566Pro)	12
chr4:55962545	T	TG	43.46	KDR	c.2615-36A>CA	rs34085292	p.?	
chr4:55972974	T	A	51.35	KDR	c.1416A>T	rs1870377 COSM149673	p. (Gln472His)	11
chr4:55980239	C	T	98.35	KDR	c.798+54G>A	rs7692791	p.?	
chr5:112175769	CGG	CAG	CAG=100	APC	c.4479G>A	COSM3760869	p. (Thr1493Thr)	16
chr5:149433596	TG	GA	100	CSF1R, HMGXB3	c.*1841TG>GA, c.2954_ 2955delCAinsTC	rs2066934	p.?	
chr7:55249063	G	A	71.04	EGFR, EGFR-AS1	c.2361G>A	rs1050171	p. (Gln787Gln)	20
rs1800861	G	T	100	RET	c.2307G>T	COSM4418405	p. (Leu769Leu)	13
chr11:534242	A	G	49.07	HRAS	c.81T>C	rs12628	p. (His27His)	2
chr13:28608280	A	G	53.5	FLT3	c.1776T>C	Novel	p. (Val592Val)	14
chr13:28610183	A	G	100	FLT3	c.1310-3T>C	rs2491231	p.?	
chr17:7579472	G	C	C=47.94	TP53	c.215C>G	rs1042522	p. (Pro72Arg)	4
chr18:48591923	T	C	63.63	SMAD4	c.1086T>C	rs1801250	p. (Phe362Phe)	9
chr22:24176287	G	A	52.5	DERL3, SMARCB1	c.1119-41G>A, c.*727C>T	rs5030613	p.?	4

Table 3. Sequencing quality of variants found in the grade III ependymoma.

Genes	Coding	Allele Coverage	Allele Ratio	p-value	FATHMM predication	Phred Score	Coverage (x)
IDH1	c.395G>A	CG=1900, TG=96	CG=0.9519, TG=0.0481	0.00001	Pathogenic	221.064	1996
ERBB4	c.421+58A>G	C=1988	C=1.0	0.00001	NA	31774.6	1988
PIK3CA	c.352+40A>G	A=1038, G=957	A=0.5203, G=0.4797	0.00001	NA	9501.82	1995
PIK3CA	c.1173A>G	A=915, G=1085	A=0.4575, G=0.5425	0.00001	Benign	11555.8	2000
FGFR3	c.1953G>A	A=1993	A=1.0	0.00001	Benign	31840.6	1993
PDGFRA	c.1701A>G	AGCCCGGATGGACATG=1941	AGCCCGGATGGACATG=1.0	0.00001	Benign	35066.6	1941
KDR	c.2615-36A>CA	T=1124, TG=864	T=0.5654, TG=0.4346	0.00001	NA	5173.27	1988
KDR	c.1416A>T	T=971, A=1025	T=0.4865, A=0.5135	0.00001	Benign	10583.1	1996
KDR	c.798+54G>A	C=33, T=1965	C=0.0165, T=0.9835	0.00001	NA	30286.5	1998
APC	c.4479G>A	CAG=1985,	CAG=1.0	0.00001	Benign	35885.9	1985
CSF1R, HMGXB3	c.*1841TG>GA, c.2954_2955delCAinsTC	GA=1977	GA=1.0	0.00001	Benign	31540.7	1977
EGFR, EGFR-AS1	c.2361G>A	G=579, A=1420	G=0.2896, A=0.7104	0.00001	Benign	17657.6	1999
RET	c.2307G>T	T=1996	T=1.0	0.00001	Benign	31993.7	1996
HRAS	c.81T>C	A=1018, G=981	A=0.5093, G=0.4907	0.00001	Benign	11998.4	1999
FLT3	c.1776T>C	A=929, G=1069	A=0.465, G=0.535	0.00001	NA	11295.9	1998
FLT3	c.1310-3T>C	G=1998	G=1.0	0.00001	Benign	32026.3	1998
TP53	c.215C>G	G=1038, C=956	G=0.5206, C=0.4794	0.00001	Benign	11559.2	1994
SMAD4	c.1086T>C	T=727, C=1272	T=0.3637, C=0.6363	0.00001	Benign	14836.6	1999
DERL3, SMARCB1	c.1119-41G>A, c.*727C>T	G=950, A=1050	G=0.475, A=0.525	0.00001	NA	13246.6	2000

(100%, 50%, and 0% in grade I, II and III, respectively)[23]. The tumor in our case is grade III anaplastic ependymoma and it stained negatively for EGFR, confirming this observation. Based upon the expression profiles of numerous angiogenesis genes (HIF-1a signaling, VEGF signaling, cell migration) and signaling pathway genes (PDGF signaling, MAPK signaling, EGFR signaling), posterior fossa ependymomas are subdivided into two groups[19]. In this case, a diagnosis of anaplastic ependymoma (WHO grade III) was made upon the observation of the above characteristics for the tumor. The pathology of the resected tissue demonstrated a hypercellular tumor with areas of perivascular pseudo rosettes, consistent with a diagnosis of ependymoma.

Despite several investigations, the correlation between histological grading of ependymoma tumors and their prognosis is unclear[8,34,38]. Apart from histopathological grading, previous studies have focused on gross deletions and chromosomal abnormalities through cytogenetic studies and array-CGH profiling of ependymomas[39,40]. These studies helped to distinguish between intracranial and spinal cord ependymomas. Around 70% of supratentorial ependymas are known to carry a fusion gene which produces the C11orf95/RELA fusion transcript and the prognosis is poor for this tumor[41]. Ion Torrent PGM sequencing

of a grade II ependymoma demonstrated MET and ATRX copy number gain[25]. Overexpression of L1 cell adhesion molecule (L1CAM), 1q25 copy number gain and a homozygous deletion in CDKN2A was also reported in some aggressive supratentorial ependymomas[42]. However, in the present case we did not detect any MET or CDKN2A mutations using the Ion AmpliSeq Cancer HotSpot panel.

In the cancer genome atlas (TCGA) projects top mutated cancer genes were IDH1, TP53, EGFR, PIK3CA, and PDGFRA (cBioportal data base, https://www.cbioportal.org). The specific variants we found in the present ependymoma case such as in TP53, HRAS, SMAD4, PIK3CA are not in TCGA projects. However, genes that are mutated in this ependymoma tumor such as IDH1, TP53, and EGFR are in top 20 mutated cancer genes with high functional impact, other genes were not in top 20 genes in ICGC data portal (https://dcc.icgc.org). In the integrative onco-genomics data base (https://www.intogen.org/search?cancer) genes mutated such as, TP53 and PDGFRA are in high-grade glioma data from St. Jude children's research hospital (HGG_D_STJUDE), and IDH1, TP53, PIK3CA and EGFR, are most recurrently mutated cancer driver genes in GBM_TCGA dataset. Also, under 'ependymoma' only search, two cohorts are found, with total 94 samples. In the
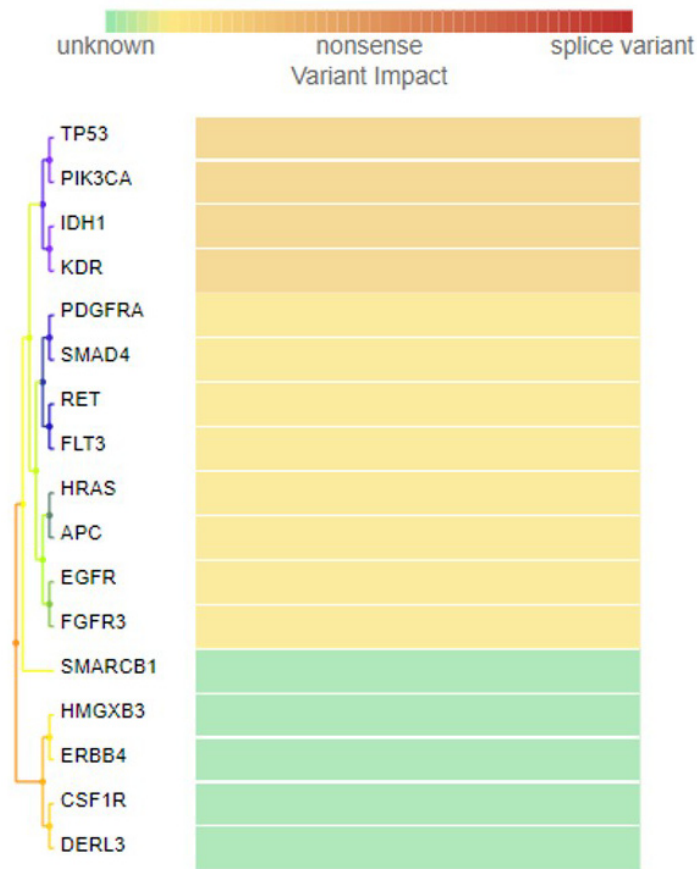
Figure 7. Heat Map showing variant impact of each gene detected in the ependymal tumor. Variant impact takes into account the type of mutation (such as insertion, deletion or frame shift) and considers the location of the variant (intronic or exonic). The color gradation from green to red indicates unknown, synonymous, missense, nonsense and splice variants, calculated based upon their SIFT, PolyPhen2 and Grantham scores.

ependymoma – DKFZ cohort, (EPD_PRY_DKFZ_2017), total 55 samples are found. The *IDH1* variant found in our case also detected as a mutational cancer driver in this cohort[43]. Ependymoma data from St. Jude children's research hospital have 39 samples, and by WGS, *PIK3CA* is detected as a mutational cancer driver in the ependymoma cohort in 2 out of 39 (5.13%) samples (3:179203765: T>A; AA345, 3:179221147: A>C, AA726), were found to have mutation in this driver gene[41].

Patients with neurofibromatosis type 2 are predisposed to the development of ependymomas, and the gene for neurofibromatosis type 2 (*NF2*) maps to chromosome 22 (q1216,17). Mutations in the *NF2* gene are uncommon in sporadic ependymomas and appear to be restricted to spinal tumors[44]. For spinal cord ependymomas, four out of eight tumors were found to have an *NF2* mutation and all eight tumors had loss of heterozygosity (LOH) of chromosome 22, where the *NF2* locus is found. However, five out of eight intracranial tumors exhibited LOH of chromosome 22 but no *NF2* mutations[24]. A high rate of truncating mutations such as nonsense and frameshift mutations in the *NF2* gene were also reported previously in spinal ependymomas[45,46]. Unfortunately, in the Ion AmpliSeq

cancer HotSpot panel primer pool used in the present study NF2 gene was not included. The *SMARCB1* germline mutations contribute to 10% of sporadic schwannomatosis. The SNP (rs5030613) found by us in this gene c.1119-41G>A is also reported in Schwannomatosis[47]. However, this SNP was not reported previously in ependymomas.

We have verified all mutations in various databases (COSMIC, ExAc and dbSNP) to confirm whether variants are novel. Only one detected in our case, a synonymous variant found in *FLT3* (c.1776T>C; p.(Val592Val), is a novel variant. In 924 glioma cases tested *FLT3* mutations found in 26 cases, a mutation in Val592 codon [c.1774G>A; p.(V592I)] was reported in 2 cases of astrocytoma grade IV. In this cohort 16 ependymoma case were included but their mutation status for *FLT3* is negative[48]. Identification of this novel variant in exon 14 of *FLT3* does not have any structural functional impact as this is a synonymous variant coding for the same amino acid. However, this variant is not reported in COSMIC database or dbSNP also. In the Leiden open variation database (LOVD) 5 more synonymous mutations were reported in exon 14 (in the juxta membrane domain amino acids 572-609); in c.1746, c.1770, c.1773, c.1803 and in codon

1815 http://databases.lovd.nl/whole_genome/variants/FLT3. The *IDH1* mutation c.395G>A; p.(Arg132His) we detected in this tumor is a substitution missense mutation which has been reported previously (COSM28746) in glioma tumors[49]. In this codon, another missense G>T mutation (COSM28750), and a compound substitution c.394_395CG>GT (COSM28751) are also known. Somatic *IDH1* mutations in this codon have been found with greater frequency in diffuse astrocytomas, oligodendrogliomas, oligoastrocytomas and secondary glioblastomas. And in anaplastic ependymoma grade III this variant is reported with 14.3% frequency[50]. However, several grade II and grade III ependymal tumors tested did not show this mutation in the *IDH1* gene[51]. For astrocytic tumors, the presence of this mutation is known to be associated with younger patients[52]. This observation supports our findings for this ependymoma tumor as the patient is six years-old. This mutation is pathogenic, having a FATHMM score of 0.94. Other variants detected in this tumor, such as those in *FGFR3*, *PDGFRA*, *KDR* (c.1416A>T), *CSF1R*, *EGFR*, *RET*, *HRAS*, *PIK3CA*, *FLT3* (c.1310-3T>C), and *SMAD4*, are benign. The *FLT3* splice variant c.1310-3T>C (rs2491231) was reported in 84% of triple negative breast cancer cases[53]. This variant was not reported in ependymoma tumors previously, this is the first time we report it here. Variants detected in this tumor have also been reported in other cancers: *PDGFRA* mutations in cervical adeno-squamous carcinomas; *ERBB4* mutations in lung adenocarcinomas; *FGFR3* mutations in breast, endometrial and ovarian cancers; *CSF1R* mutations in prostate cancer; *EGFR* mutations in lung adenocarcinomas; *RET* mutations in thyroid carcinomas; *HRAS* mutations in melanomas; and *SMAD4* mutations in breast cancer. However, with the exception of the *KDR* variant c.1416A>T, this is the first time the above variants are reported in a brain tumor[54–62].

We found an intronic variant in *PIK3CA* and one missense mutation in this gene. This missense mutation was also reported previously in hemangioblastoma and in colon adenocarcinoma[63,64]. Missense mutations in *PIK3CA* are known to promote glioblastoma tumor progression[65]. Mutations of the *PTEN* gene are rare in ependymomas and we have also not detected any *PTEN* mutations in this tumor[66]. The *KDR (VEGFR2)* gene plays an important role in neovascularization and tumor initiation by glioma stem-like cells[67]. In non-small cell lung cancer patients, the Gln472His SNP is associated with increased *KDR* activity, and was correlated with increased micro vessel density[68]. This variant was not known in ependymoma tumors previously. This mutation is reported in Colo-rectal cancer, melanoma, non-small cell lung cancer, and it's an important target for drugs like Avastin (Bevacizumab), Aflibrcept, and drugs reported in (http://atlasgeneticsoncology.org/Genes/GC_KDR.html).

Mutations in cancer driver genes such as *TP53*, *CDKN2A*, and *EGFR*, which are frequently affected in gliomas, have been shown to be rare in ependymomas[44,66,69]. We have detected a *TP53* mutation (c.215C>G, p.Pro72Arg, rs1042522) in this tumor with a frequency of 47.94%. This mutation p.(Pro72Arg) has also been reported previously in a medulloblastoma tumor in a young patient[70]. Previous studies have shown that out of 15 ependymoma tumors tested, only one case, a patient with a

malignant ependymoma of the posterior fossa, had a mutation in exon 6 of the *TP53* gene, which was silent, and in another study only one out of 31 ependymoma tumors tested contained a mutation in the *TP53* gene[71,72]. However, in another study, out of 15 ependymoma tumors, none had a mutation in the *TP53* gene, suggesting that this gene does not play an important role in the pathogenesis and development of ependymomas, unlike other brain tumor types[66,72,73]. Miller *et al.*, (2018) through whole-exome sequencing of an anaplastic ependymoma tumor, have shown mutations in several cancer-related genes, as well as genes related to metabolism, neuro-developmental disorder, epigenetic modifiers and intracellular signaling[74]. These authors have shown resistance-promoting variant expression in a single ependymoma case at different stages of recurrence. However, these genes were not present in the cancer panel we used in this study. Using the human exome capture on Illumina, Bettegowda *et al.*, (2013) have reported that in one out of eight grade III intracranial ependymomas, tumors have mutations in *PTEN* and *TP53*, and one tumor with *HIST1H3C* mutations[24]. The *HIST1H3C* p.(Lys27Met) mutation has also been reported previously in posterior fossa ependymomas[75]. Ependymomas may in fact represent a very heterogeneous class of tumors, each with distinct molecular profiles and, even within posterior fossa ependymomas, there are at least two distinct gene expression patterns, as demonstrated by Witt *et al.*, (2011)[19,76]. Overall, in previous studies, a very low frequency of mutations was observed in both intracranial and spinal ependymomas and our findings also supports this observation[19,24,25,41].

The Ion AmpliSeq Cancer HotSpot Panel consists of 207 primers in 1 tube, targeting 50 oncogenes and tumor suppressor genes that are frequently mutated in several types of cancers. The detected mutations were found to have high accuracy; 100% amplicons had at least 500 reads and 500x target base coverage was also 100%. This high level of accuracy and the high depth of coverage achieved with the Ion Proton system allowed us to reliably detect low frequency mutations with high confidence. Allele coverage in most of the variants is around 2000x, the p-value was 0.00001 and the Phred score was very high for all the variants, indicating high confidence in the variants found in this tumor. Apart from its use in whole-exome sequencing, cancer panel analysis has also become common practice for Ion Proton[26]. The Ion Proton instrument has the advantage of pooling samples using barcodes and the Ion PI chip. For pooled samples, sequencing enables a high throughput up to 15 Gb of data, with more than 60–80 million reads passing read filtering. The purpose of read filtering is to discard the reads that contain low quality sequences, to remove polyclonal reads, remove reads with an off-scale signal, remove reads lacking a sequencing key, remove adapter dimers, and remove short reads etc. If the computed mean read length from all the reads and the minimum total mapped reads in the sample is less than the specified threshold, that sample does not pass the quality control.

Recent molecular diagnostics research had helped in subdividing glioblastomas, oligodendrogliomas and oligoastrocytomas into genetically diverse groups of tumors, and these mutational markers may help in predicting the prognosis and response to therapy[77]. However, such a strategy for the molecular

subdivision of ependymomas has been not successful so far using mutational profiling. Epigenetic markers and fusion protein analysis have also helped in identifying new groups of supratentorial ependymoma tumors and in spite of the histopathological signs of malignancy, a small set of ependymomas had a very good prognosis, suggesting that this subgroup of tumors should not be diagnosed as classic ependymomas[78]. However, another study showed that methylation profiling did not identify a consistent molecular class within the supratentorial tumors, but successfully sub-classified posterior fossa ependymoma into two subgroups[79].

In conclusion, we have identified four known missense mutations, eight synonymous and seven intronic, in this grade III ependymoma. Out of these, only one mutation in *FLT3* (c.1776T>C, synonymous) is novel, and only one mutation in *IDH1* (c.395G>A, missense) is deleterious, with all other mutations benign. Many of the variants we reported here were not detected in the ependymal tumors analyzed by NGS previously. *HRAS* c.81T>C, *PIK3CA* c.1173A>G, *RET* c.2307G>T, *KDR* c.1416A>T, *APC* c.4479G>A, *EGFR* c.2361G>A and *FLT3* c.1310-3T>C variants have not been previously reported in brain tissue, as verified in COSMIC data base, although they have been reported in other tissues like lung and breast. Further studies are warranted, using NGS methods in all three grades of intracranial ependymomas to identify the genetic signatures that may distinguish between these tumors at the molecular genetic level.

Data availability
Underlying data
Raw sequence reads for this tumor on Sequence Read Archive, Accession number SRP192752: https://identifiers.org/insdc.sra/SRP192752

Open Science Framework: Mutation profiling of anaplastic ependymoma grade III by Ion Proton next generation DNA sequencing. https://doi.org/10.17605/osf.io/y9sfg[33]

This project contains the following underlying data:

- All variants before filteration.xlsx (spreadsheet of all annotated variants)

- Final Variant Calls using HotSpot filter.xlsx (spreadsheet of annotated variants called using HotSpot filter)

- TSVC_variants_IonXpress_013.vcf (file containing all variants (un-annotated) in vcf format)

- TSVC_variants_IonXpress_013.vcf.gz.tbi (file containing all variants (un-annotated) in vcf.gz.tbi format)

- heatmap-gr3 ion rep.csv (spreadsheet containing impact scores used to generate heat map)

- EGFR Figure neg.jpg (images for EGFR staining)

- Fig2A.jpg – Figur4D.jpg (raw image files used in Figure 2–Figure 5)

- Radiology Fig.1.jpg – Radiology Figure 1 (2).jpg (raw image files used in Figure 1)

Data are available under the terms of the Creative Commons Attribution 4.0 International license (CC-BY 4.0).

Extended data
Open Science Framework: Mutation profiling of anaplastic ependymoma grade III by Ion Proton next generation DNA sequencing. https://doi.org/10.17605/osf.io/y9sfg[33]

This project contains the following extended data:

- Gr-3 Advaiata Final report.pdf (Advaiata iVariant analysis report)

Data are available under the terms of the Creative Commons Attribution 4.0 International license (CC-BY 4.0).

References

1. Duff DJ, Miller DC: **Ependymomas (Review).** *AJSP: Reviews & Reports.* 2013; **18**(5): 221–230.
   Publisher Full Text

2. Wu J, Armstrong TS, Gilbert MR: **Biology and management of ependymomas.** *Neuro Oncol.* 2016; **18**(7): 902–913.
   PubMed Abstract | **Publisher Full Text** | **Free Full Text**

3. Wesseling P, Capper D: **WHO 2016 Classification of gliomas.** *Neuropathol Appl Neurobiol.* 2018; **44**(2): 139–150.
   PubMed Abstract | **Publisher Full Text**

4. Ostrom QT, Gittleman H, Fulop J, *et al.*: **CBTRUS Statistical Report: Primary Brain and Central Nervous System Tumors Diagnosed in the United States in 2008-2012.** *Neuro Oncol.* 2015; **17 Suppl 4**: iv1–iv62.
   PubMed Abstract | **Publisher Full Text** | **Free Full Text**

5. Zamora C, Huisman TA, Izbudak I: **Supratentorial Tumors in Pediatric Patients.** *Neuroimaging Clin N Am.* 2017; **27**(1): 39–67.
   PubMed Abstract | **Publisher Full Text**

6. Kilday JP, Rahman R, Dyer S, *et al.*: **Pediatric ependymoma: biological perspectives.** *Mol Cancer Res.* 2009; **7**(6): 765–786.
   PubMed Abstract | **Publisher Full Text**

7. Hamilton RL, Pollack IF: **The molecular biology of ependymomas.** *Brain Pathol.* 1997; **7**(2): 807–822.
   PubMed Abstract | **Publisher Full Text**

8. Horn B, Heideman R, Geyer R, *et al.*: **A multi-institutional retrospective study of intracranial ependymoma in children: identification of risk factors.** *J Pediatr Hematol Oncol.* 1999; **21**(3): 203–211.
   PubMed Abstract | **Publisher Full Text**

9.   Spoto GP, Press GA, Hesselink JR, *et al.*: **Intracranial ependymoma and subependymoma: MR manifestations.** *AJR Am J Roentgenol.* 1990; **154**(4): 837–845.
     PubMed Abstract | **Publisher Full Text**

10. Andrade FG, de Aguiar PH, Matushita H, *et al.*: **Intracranial and spinal ependymoma: series at Faculdade de Medicina, Universidade de São Paulo.** *Arq Neuropsiquiatr.* 2009; **67**(3A): 626–632.
     PubMed Abstract | **Publisher Full Text**

11. Vera-Bolanos E, Aldape K, Yuan Y, *et al.*: **Clinical course and progression-free survival of adult intracranial and spinal ependymoma patients.** *Neuro Oncol.* 2015; **17**(3): 440–447.
     PubMed Abstract | **Publisher Full Text** | **Free Full Text**

12. Milano MT, Johnson MD, Sul J, *et al.*: **Primary spinal cord glioma: a Surveillance, Epidemiology, and End Results database study.** *J Neurooncol.* 2010; **98**(1): 83–92.
     PubMed Abstract | **Publisher Full Text**

13. Louis DN, Perry A, Reifenberger G, *et al.*: **The 2016 World Health Organization Classification of Tumors of the Central Nervous System: a summary.** *Acta Neuropathol.* 2016; **131**(6): 803–820.
     PubMed Abstract | **Publisher Full Text**

14. Leeper H, Felicella MM, Walbert T: **Recent Advances in the Classification and Treatment of Ependymomas.** *Curr Treat Options Oncol.* 2017; **18**(9): 55.
     PubMed Abstract | **Publisher Full Text**

15. Hirose Y, Aldape K, Bollen A, *et al.*: **Chromosomal abnormalities subdivide ependymal tumors into clinically relevant groups.** *Am J Pathol.* 2001; **158**(3): 1137–1143.
     PubMed Abstract | **Publisher Full Text** | **Free Full Text**

16. Ross GW, Rubinstein LJ: **Lack of histopathological correlation of malignant ependymomas with postoperative survival.** *J Neurosurg.* 1989; **70**(1): 31–36.
     PubMed Abstract | **Publisher Full Text**

17. Pajtler KW, Witt H, Sill M, *et al.*: **Molecular Classification of Ependymal Tumors across All CNS Compartments, Histopathological Grades, and Age Groups.** *Cancer Cell.* 2015; **27**(5): 728–43.
     PubMed Abstract | **Publisher Full Text** | **Free Full Text**

18. Palm T, Figarella-Branger D, Chapon F, *et al.*: **Expression profiling of ependymomas unravels localization and tumor grade-specific tumorigenesis.** *Cancer.* 2009; **115**(17): 3955–3968.
     PubMed Abstract | **Publisher Full Text**

19. Witt H, Mack SC, Ryzhova M, *et al.*: **Delineation of two clinically and molecularly distinct subgroups of posterior fossa ependymoma.** *Cancer Cell.* 2011; **20**(2): 143–157.
     PubMed Abstract | **Publisher Full Text** | **Free Full Text**

20. Korshunov A, Neben K, Wrobel G, *et al.*: **Gene expression patterns in ependymomas correlate with tumor location, grade, and patient age.** *Am J Pathol.* 2003; **163**(5): 1721–1727.
     PubMed Abstract | **Publisher Full Text** | **Free Full Text**

21. Mazewski C, Soukup S, Ballard E, *et al.*: **Karyotype studies in 18 ependymomas with literature review of 107 cases.** *Cancer Genet Cytogenet.* 1999; **113**(1): 1–8.
     PubMed Abstract | **Publisher Full Text**

22. Ward S, Harding B, Wilkins P, *et al.*: **Gain of 1q and loss of 22 are the most common changes detected by comparative genomic hybridisation in paediatric ependymoma.** *Genes Chromosomes Cancer.* 2001; **32**(1): 59–66.
     PubMed Abstract | **Publisher Full Text**

23. Ferguson SD, Zhou S, Xiu J, *et al.*: **Ependymomas overexpress chemoresistance and DNA repair-related proteins.** *Oncotarget.* 2018; **9**(8): 7822–7831.
     PubMed Abstract | **Publisher Full Text** | **Free Full Text**

24. Bettegowda C, Agrawal N, Jiao Y, *et al.*: **Exomic sequencing of four rare central nervous system tumor types.** *Oncotarget.* 2013; **4**(4): 572–583.
     PubMed Abstract | **Publisher Full Text** | **Free Full Text**

25. Nikiforova MN, Wald AI, Melan MA, *et al.*: **Targeted next-generation sequencing panel (GlioSeq) provides comprehensive genetic profiling of central nervous system tumors.** *Neuro Oncol.* 2016; **18**(3): 379–387.
     PubMed Abstract | **Publisher Full Text** | **Free Full Text**

26. Mehrotra M, Duose DY, Singh RR, *et al.*: **Versatile ion S5XL sequencer for targeted next generation sequencing of solid tumors in a clinical laboratory.** *PLoS One.* 2017; **12**(8): e0181968.
     PubMed Abstract | **Publisher Full Text** | **Free Full Text**

27. Li H: **A statistical framework for SNP calling, mutation discovery, association mapping and population genetical parameter estimation from sequencing data.** *Bioinformatics.* 2011; **27**(21): 2987–93.
     PubMed Abstract | **Publisher Full Text** | **Free Full Text**

28. Koboldt DC, Chen K, Wylie T, *et al.*: **VarScan: variant detection in massively parallel sequencing of individual and pooled samples.** *Bioinformatics.* 2009; **25**(17): 2283–5.
     PubMed Abstract | **Publisher Full Text** | **Free Full Text**

29. Cingolani P, Platts A, Wang le L, *et al.*: **A program for annotating and predicting the effects of single nucleotide polymorphisms, SnpEff: SNPs in the genome of Drosophila melanogaster strain w[1118]; iso-2; iso-3.** *Fly (Austin).* 2012; **6**(2): 80–92.
     PubMed Abstract | **Publisher Full Text** | **Free Full Text**

30. Cingolani P, Patel VM, Coon M, *et al.*: **Using *Drosophila melanogaster* as a Model for Genotoxic Chemical Mutational Studies with a New Program, SnpSift.** *Front Genet.* 2012; **3**: 35.
     PubMed Abstract | **Publisher Full Text** | **Free Full Text**

31. Shihab HA, Gough J, Cooper DN, *et al.*: **Predicting the functional, molecular, and phenotypic consequences of amino acid substitutions using hidden Markov models.** *Hum Mutat.* 2013; **34**(1): 57–65.
     PubMed Abstract | **Publisher Full Text** | **Free Full Text**

32. Grantham R: **Amino acid difference formula to help explain protein evolution.** *Science.* 1974; **185**(4154): 862–864.
     PubMed Abstract | **Publisher Full Text**

33. Taher MM, Butt ME, Alyami SH, *et al.*: **Mutation profiling of anaplastic ependymoma grade III by Ion Proton next generation DNA sequencing.** 2019.
     http://www.doi.org/10.17605/OSF.IO/Y9SFG

34. Raghunathan A, Wani K, Armstrong TS, *et al.*: **Histological predictors of outcome in ependymoma are dependent on anatomic site within the central nervous system.** *Brain Pathol.* 2013; **23**(5): 584–594.
     PubMed Abstract | **Publisher Full Text**

35. Kuncova K, Janda A, Kasal P, *et al.*: **Immunohistochemical prognostic markers in intracranial ependymomas: systematic review and meta-analysis.** *Pathol Oncol Res.* 2009; **15**(4): 605–614.
     PubMed Abstract | **Publisher Full Text**

36. Tena-Suck ML, Castillejos-Lopez M, Diaz-Alba A, *et al.*: **Expression of glial acidic fibrillary protein delta and E-cadherin in ependymomas; clinic-pathological and immunohistochemistry correlation.** *J Histol Histopath.* 2015; **2**: Article 17.
     Publisher Full Text

37. Gumbiner BM: **Regulation of cadherin-mediated adhesion in morphogenesis.** *Nat Rev Mol Cell Biol.* 2005; **6**(8): 622–634.
     PubMed Abstract | **Publisher Full Text**

38. Figarella-Branger D, Civatte M, Bouvier-Labit C, *et al.*: **Prognostic factors in intracranial ependymomas in children.** *J Neurosurg.* 2000; **93**(4): 605–613.
     PubMed Abstract | **Publisher Full Text**

39. Dyer S, Prebble E, Davison V, *et al.*: **Genomic imbalances in pediatric intracranial ependymomas define clinically relevant groups.** *Am J Pathol.* 2002; **161**(6): 2133–2141.
     PubMed Abstract | **Publisher Full Text** | **Free Full Text**

40. Sainati L, Montaldi A, Putti MC, *et al.*: **Cytogenetic t(11;17)(q13;q21) in a pediatric ependymoma. Is 11q13 a recurring breakpoint in ependymomas?** *Cancer Genet Cytogenet.* 1992; **59**(2): 213–216.
     PubMed Abstract | **Publisher Full Text**

41. Parker M, Mohankumar KM, Punchihewa C, *et al.*: ***C11orf95-RELA* fusions drive oncogenic NF-κB signalling in ependymoma.** *Nature.* 2014; **506**(7489): 451–455.
     PubMed Abstract | **Publisher Full Text** | **Free Full Text**

42. Kim SI, Lee Y, Kim SK, *et al.*: **Aggressive Supratentorial Ependymoma, *RELA* Fusion-Positive with Extracranial Metastasis: A Case Report.** *J Pathol Transl Med.* 2017; **51**(6): 588–593.
     PubMed Abstract | **Publisher Full Text** | **Free Full Text**

43. Grobner SN, Worst BC, Weischenfeldt J, *et al.*: ICGC PedBrain-Seq Project; ICGC MMML-Seq Project. **The Landscape of Genomic Alterations Across Childhood Cancers.** *Nature.* 2018; **555**(7696): 321–327.
     PubMed Abstract | **Publisher Full Text**

44. von Haken MS, White EC, Daneshvar-Shyesther L, *et al.*: **Molecular genetic analysis of chromosome arm 17p and chromosome arm 22q DNA sequences in sporadic pediatric ependymomas.** *Genes Chromosom Cancer.* 1996; **17**(1): 37–44.
     PubMed Abstract | **Publisher Full Text**

45. Rubio MP, Correa KM, Ramesh V, *et al.*: **Analysis of the neurofibromatosis 2 gene in human ependymomas and astrocytomas.** *Cancer Res.* 1994; **54**(1): 45–47.
     PubMed Abstract

46. Plotkin SR, O'Donnell CC, Curry WT, *et al.*: **Spinal ependymomas in neurofibromatosis Type 2: a retrospective analysis of 55 patients.** *J Neurosurg Spine.* 2011; **14**(4): 543–547.
     PubMed Abstract | **Publisher Full Text**

47. Rousseau G, Noguchi T, Bourdon V, *et al.*: **SMARCB1/INI1 germline mutations contribute to 10% of sporadic schwannomatosis.** *BMC Neurol.* 2011; **11**: 9.
     PubMed Abstract | **Publisher Full Text** | **Free Full Text**

48. Zehir A, Benayed R, Berger MF, *et al.*: **Mutational landscape of metastatic cancer revealed from prospective clinical sequencing of 10,000 patients.** *Nat Med.* 2017; **23**(6): 703–713.
     PubMed Abstract | **Publisher Full Text** | **Free Full Text**

49. Wang PF, Liu N, Song HW, *et al.*: **IDH-1[R132H] mutation status in diffuse glioma patients: implications for classification.** *Oncotarget.* 2016; **7**(21): 31393–400.
     PubMed Abstract | **Publisher Full Text** | **Free Full Text**

50. Yusoff AM, Zulfakhar FN, Sul'ain MD, *et al.*: **Association of The IDH1 C.395G>A (R132H) Mutation with Histological Type in Malay Brain Tumors.** *Asian Pac J Cancer Prev.* 2016 ;**17**(12): 5195–5201.
     PubMed Abstract | **Publisher Full Text** | **Free Full Text**

51. Mellai M, Piazzi A, Caldera V, *et al.*: ***IDH1* and *IDH2* mutations, immunohistochemistry and associations in a series of brain tumors.** *J Neurooncol.* 2011; **105**(21): 345–57.
     PubMed Abstract | **Publisher Full Text**

52. Balss J, Meyer J, Mueller W, *et al.*: **Analysis of the IDH1 codon 132 mutation in brain tumors.** *Acta Neuropathol.* 2008; **116**(6): 597–602.
     PubMed Abstract | **Publisher Full Text**

53. Uscanga-Perales GI, Santuario-Facio SK, Sanchez-Dominguez CN, *et al.*:

Genetic alterations of triple negative breast cancer (TNBC) in women from Northeastern Mexico. *Oncol Lett.* 2019; **17**(12): 3581–3588.
PubMed Abstract | **Publisher Full Text** | **Free Full Text**

54. Longatto-Filho A, Pinheiro C, Martinho O, *et al.*: **Molecular characterization of EGFR, PDGFRA and VEGFR2 in cervical adenosquamous carcinoma.** *BMC Cancer.* 2009; **9**: 212.
PubMed Abstract | **Publisher Full Text** | **Free Full Text**

55. Bonfiglio S, Vanni I, Rossella V, *et al.*: **Performance comparison of two commercial human whole-exome capture systems on formalin-fixed paraffin-embedded lung adenocarcinoma samples.** *BMC Cancer.* 2016; **16**: 692.
PubMed Abstract | **Publisher Full Text** | **Free Full Text**

56. Gonzalez-Bosquet J, Calcei J, Wei JS, *et al.*: **Detection of somatic mutations by high-resolution DNA melting (HRM) analysis in multiple cancers.** *PLoS One.* 2011; **6**(1): e14522.
PubMed Abstract | **Publisher Full Text** | **Free Full Text**

57. Qu HQ, Jacob K, Fatet S, *et al.*: **Genome-wide profiling using single-nucleotide polymorphism arrays identifies novel chromosomal imbalances in pediatric glioblastomas.** *Neuro Oncol.* 2010; **12**(2): 153–63.
PubMed Abstract | **Publisher Full Text** | **Free Full Text**

58. Lo Iacono M, Buttigliero C, Monica V, *et al.*: **Retrospective study testing next generation sequencing of selected cancer-associated genes in resected prostate cancer.** *Oncotarget.* 2016; **7**(12): 14394–14404.
PubMed Abstract | **Publisher Full Text** | **Free Full Text**

59. Leichsenring J, Volckmar AL, Magios N, *et al.*: **Synonymous EGFR variant p.Q787Q is neither prognostic nor predictive in patients with lung adenocarcinoma.** *Genes Chromosomes Cancer.* 2017; **56**(3): 214–220.
PubMed Abstract | **Publisher Full Text**

60. Ceolin L, Siqueira DR, Romitti M, *et al.*: **Molecular basis of medullary thyroid carcinoma: the role of *RET* polymorphisms.** *Int J Mol Sci.* 2012; **13**(1): 221–39.
PubMed Abstract | **Publisher Full Text** | **Free Full Text**

61. Tomei S, Adams S, Uccellini L, *et al.*: **Association between *HRAS* rs12628 and rs112587690 polymorphisms with the risk of melanoma in the North American population.** *Med Oncol.* 2012; **29**(5): 3456–3461.
PubMed Abstract | **Publisher Full Text** | **Free Full Text**

62. Tram E, Ibrahim-Zada I, Briollais L, *et al.*: **Identification of germline alterations of the mad homology 2 domain of SMAD3 and SMAD4 from the Ontario site of the breast cancer family registry (CFR).** *Breast Cancer Res.* 2011; **13**(4): R77.
PubMed Abstract | **Publisher Full Text** | **Free Full Text**

63. Shankar GM, Taylor-Weiner A, Lelic N, *et al.*: **Sporadic hemangioblastomas are characterized by cryptic *VHL* inactivation.** *Acta Neuropathol Commun.* 2014; **2**: 167.
PubMed Abstract | **Publisher Full Text** | **Free Full Text**

64. Ashktorab H, Mokarram P, Azimi H, *et al.*: **Targeted exome sequencing reveals distinct pathogenic variants in Iranians with colorectal cancer.** *Oncotarget.* 2017; **8**(5): 7852–7866.
PubMed Abstract | **Publisher Full Text** | **Free Full Text**

65. McNeill RS, Stroobant EE, Smithberger E, *et al.*: **PIK3CA missense mutations promote glioblastoma pathogenesis, but do not enhance targeted PI3K inhibition.** *PLoS One.* 2018; **13**(7): e0200014.
PubMed Abstract | **Publisher Full Text** | **Free Full Text**

66. Duerr EM, Rollbrocker B, Hayashi Y, *et al.*: **PTEN mutations in gliomas and**

glioneuronal tumors. *Oncogene.* 1998; **16**(17): 2259–2264.
PubMed Abstract | **Publisher Full Text**

67. Yao X, Ping Y, Liu Y, *et al.*: **Vascular endothelial growth factor receptor 2 (VEGFR-2) plays a key role in vasculogenic mimicry formation, neovascularization and tumor initiation by Glioma stem-like cells.** *PLoS One.* 2013; **8**(3): e57188.
PubMed Abstract | **Publisher Full Text** | **Free Full Text**

68. Glubb DM, Cerri E, Gieseet A, *et al.*: **Novel functional germline variants in the VEGF receptor 2 gene and their effect on gene expression and microvessel density in lung cancer.** *Clin Cancer Res.* 2011; 17(16): 5257–5267.
PubMed Abstract | **Publisher Full Text** | **Free Full Text**

69. Ohgaki H, Eibl RH, Wiestler OD, *et al.*: ***p53* mutations in nonastrocytic human brain tumors.** *Cancer Res.* 1991; **51**(22): 6202–6205.
PubMed Abstract

70. Sardi I, Giunti L, Donati P, *et al.*: **Loss of heterozygosity and p53 polymorphism Pro72Arg in a young patient with medulloblastoma.** *Oncol Rep.* 2003; **10**(3): 773–775.
PubMed Abstract

71. Metzger AK, Sheffield VC, Duyk G, *et al.*: **Identification of a germ-line mutation in the p53 gene in a patient with an intracranial ependymoma.** *Proc Nat Acad Sci U S A.* 1991; **88**(17): 7825–7829.
PubMed Abstract | **Publisher Full Text** | **Free Full Text**

72. Fink KL, Rushing EJ, Schold SC Jr, *et al.*: **Infrequency of p53 gene mutations in ependymomas.** *J Neurooncol.* 1996; **27**(2): 111–115.
PubMed Abstract | **Publisher Full Text**

73. Louis DN: **The p53 gene and protein in human brain tumors.** *J Neuropathol Exp Neurol.* 1994; **53**(1): 11–21.
PubMed Abstract | **Publisher Full Text**

74. Miller CA, Dahiya S, Li T, *et al.*: **Resistance-promoting effects of ependymoma treatment revealed through genomic analysis of multiple recurrences in a single patient.** *Cold Spring Harb Mol Case Stud.* 2018; **4**(2): pii: a002444.
PubMed Abstract | **Publisher Full Text** | **Free Full Text**

75. Gessi M, Capper D, Sahm F, *et al.*: **Evidence of H3 K27M mutations in posterior fossa ependymomas.** *Acta Neuropathol.* 2016; **132**(4): 635–7.
PubMed Abstract | **Publisher Full Text**

76. Johnson RA, Wright KD, Poppleton H, *et al.*: **Cross-species genomics matches driver mutations and cell compartments to model ependymoma.** *Nature.* 2010; **466**(7306): 632–636.
PubMed Abstract | **Publisher Full Text** | **Free Full Text**

77. Park SH, Won J, Kim SI, *et al.*: **Molecular Testing of Brain Tumor.** *J Pathol Transl Med.* 2017; **51**(3): 205–223.
PubMed Abstract | **Publisher Full Text** | **Free Full Text**

78. Pagès M, Pajtler KW, Puget S, *et al.*: **Diagnostics of pediatric supratentorial RELA ependymomas: integration of information from histopathology, genetics, DNA methylation and imaging.** *Brain Pathol.* 2019; **29**(3): 325–335.
PubMed Abstract | **Publisher Full Text**

79. Fukuoka K, Kanemura Y, Shofuda T, *et al.*: **Significance of molecular classification of ependymomas: *C11orf95-RELA* fusion-negative supratentorial ependymomas are a heterogeneous group of tumors.** *Acta Neuropathol Commun.* 2018; **6**(1): 134.
PubMed Abstract | **Publisher Full Text** | **Free Full Text**

Open Peer Review

Current Peer Review Status: ✔ ✔

Version 2

Reviewer Report 25 June 2020

✔ **Luni Emdad**

Department of Human and Molecular Genetics, School of Medicine, Virginia Commonwealth University, Richmond, VA, USA

Authors have addressed my previous comments, no additional comments are noted.

Competing Interests: No competing interests were disclosed.

Reviewer Expertise: Cancer Biology and Molecular Oncology, Genetics, Targeted experimental therapeutics development

I confirm that I have read this submission and believe that I have an appropriate level of expertise to confirm that it is of an acceptable scientific standard.

Version 1

Reviewer Report 26 February 2020

✔ **Firoz Ahmad**

Research and Development Division, SRL Ltd, Mumbai, Maharashtra, India

The authors presented report on their NGS study on anaplastic ependymoma grade III by Ion Proton next generation DNA sequencing.

The article looks interesting, and is well written. Since this report is from a single case, a necessary correction has to be made in the material section. Also, the authors need to mention the tumor content of the FFPE block which was taken for the NGS analysis.

I feel, the author need to cut down on the text significantly while explaining NGS data analysis and variant identification statistics. There is too much of information which is not required. The authors have already shared the coverage analysis report which is sufficient.

Except for IDH1 mutation, other variants are non significant and hence do not add much value clinically. Identification of *FLT3* p.(Val592Val) does not carry any meaning unless and until the authors show the functional impact of this variant.

Overall, good article but the text needs to be significantly cut down considering this to be a single case report.

Is the work clearly and accurately presented and does it cite the current literature?
Partly

Is the study design appropriate and is the work technically sound?
Yes

Are sufficient details of methods and analysis provided to allow replication by others?
Yes

If applicable, is the statistical analysis and its interpretation appropriate?
Yes

Are all the source data underlying the results available to ensure full reproducibility?
Yes

Are the conclusions drawn adequately supported by the results?
Partly

Competing Interests: No competing interests were disclosed.

Reviewer Expertise: Molecular Diagnostics, Cancer Genetics, Next Generation Sequencing.

I confirm that I have read this submission and believe that I have an appropriate level of expertise to confirm that it is of an acceptable scientific standard.

Author Response 09 Jun 2020

Mohiuddin Taher, Umm-Al-Qura University, Makkah, Saudi Arabia

Response to 2nd Reviewer's Comments:

We are thankful to this reviewer (Dr. Firoz Ahmed, Research Scientist, and Senior Manager-R&D, SRL Diagnostics, SRL Limited, Goregaon (West), Mumbai, India) for the helpful suggestions and comments. We have made the necessary changes in the manuscript following these suggestions.

Our answers to the comments are listed below.

Comment:
The article looks interesting and is well written. Since this report is from a single case, a necessary correction has to be made in the material section. Also, the authors need to mention the tumor content of the FFPE block which was taken for the NGS analysis.

Answer:

We agree with the reviewer's suggestion about the sample size. Regarding the single case, a correction is made in the manuscript in the Methods section.

As suggested by the reviewer, we have indicated tumor tissue content of the FFPE block used in this investigation (Methods section).

Comment:
I feel the author needs to cut down on the text significantly while explaining NGS data analysis and variant identification statistics. There is too much of information which is not required. The authors have already shared the coverage analysis report which is sufficient.

Answer:

We agree with the reviewer's suggestion, however, according to the journal's policy, we have described in detail manner several techniques used in this study and the results also in detail. The NGS data analysis such as variant identification and coverage analysis will be helpful to reproduce this work and help others to understand the data who are not familiar with NGS analysis.

Comment:
Except for *IDH1* mutation, other variants are non-significant and hence do not add much value clinically. Identification of *FLT3* p. (Val592Val) does not carry any meaning unless and until the authors show the functional impact of this variant.

Answer:

Referee-1 also made a similar comment, and we agree with this reviewer's suggestion. We have made the necessary changes in the revised manuscript. We have identified in this study four missense variants; c.395G>A in *IDH1*, in c.1173A>G in *PIK3CA* in c.1416A>T in *KDR*, in c.215C>G in *TP53*. Other variants are synonymous and intronic ones. We agree with the reviewer's comments that "Identification of *FLT3* mutation p. (Val592Val) in exon 14 does not have any structural-functional impact as this is a synonymous variant coding for the same amino acid." However, this variant is not reported in the COSMIC database or dbSNP also. It is a novel variant of *FLT3*, so it is important to report this variant. In the LOVD database 5 more synonymous mutations were reported in exon 14 (amino acids 572-609, in the juxtamembrane domain); in c.1746, c.1770, c.1773, c.1803 and in codon 1805; http://databases.lovd.nl/whole_genome/variants/FLT3. Internal tandem duplications of *FLT3* (*FLT3*-ITD) are the most common mutations (in the juxtamembrane domain) associated with acute

myelogenous leukemia (AML) and are a prognostic indicator associated with adverse disease outcome. Activating internal tandem duplication (ITD) mutations in *FLT3* (*FLT3*-ITD) are detected in approximately 20% of acute myeloid leukemia (AML).

Competing Interests: Nil.

Reviewer Report 17 October 2019

?
Luni Emdad
Department of Human and Molecular Genetics, School of Medicine, Virginia Commonwealth University, Richmond, VA, USA

In this study authors analyzed mutation patterns by next generation sequencing (NGS) in order to determine genomic changes in an anaplastic ependymoma. Authors identified one novel synonymous mutation and one deleterious missense mutation in this grade III ependymoma.

Comments:
1. In the clinical specimen section authors state "Specimens from all patients willing to give written informed consent and diagnosed with gliomas were eligible to be included in this study." However, the specimen used in this study for NGS analysis was obtained from a single patient's tumor tissue. What are the other samples and in what study they were used?

2. Figure 2A: authors indicate yellow arrow showing palisading necrosis; is this the correct location?

3. Authors conclude they identified four known missense mutations, eight synonymous and seven intronic, in this grade III ependymoma. How global these signature molecules in the context of grade III ependymoma? Can the authors add additional correlation analysis by analyzing TCGA or other bioinformatics based data?

4. Authors indicate FLT3 (c.1776T>C, synonymous) is novel, which is interesting; is this mutation reported in other cancer than ependymoma? What is the clinical and functional significance of this mutation in ependymoma progression?

Is the work clearly and accurately presented and does it cite the current literature?
Partly

Is the study design appropriate and is the work technically sound?
Partly

Are sufficient details of methods and analysis provided to allow replication by others?
Yes

If applicable, is the statistical analysis and its interpretation appropriate?
Yes

Are all the source data underlying the results available to ensure full reproducibility?
No source data required

Are the conclusions drawn adequately supported by the results?
Partly

Competing Interests: No competing interests were disclosed.

Reviewer Expertise: Cancer Biology and Molecular Oncology, Genetics, Targeted experimental therapeutics development

I confirm that I have read this submission and believe that I have an appropriate level of expertise to confirm that it is of an acceptable scientific standard, however I have significant reservations, as outlined above.

Author Response 09 Jun 2020
Mohiuddin Taher, Umm-Al-Qura University, Makkah, Saudi Arabia

We are thankful to the reviewer-1 (Dr. Luni Emdad, Assistant Professor, Human and Molecular Genetics Department, Virginia Commonwealth University, Richmond, USA) for the helpful suggestions and comments. We have made the necessary changes in the revised manuscript following these suggestions. Our answers to the comments are listed below.
Comment:
1. In the clinical specimen, section authors state "Specimens from all patients willing to give written informed consent and diagnosed with gliomas were eligible to be included in this study." However, the specimen used in this study for NGS analysis was obtained from a single patient's tumor tissue. What are the other samples and in what study they were used?
Answer:
The present study is a part of the project on mutation profiling of brain tumors in the Saudi population which is supported by a grant from Umm-Al-Qura University (Code. No. 43509008). For this project, various gliomas such as GBM, astrocytomas, oligodendrogliomas, and ependymoma tumors (all grades) were collected. The NGS analysis is ongoing for many other tumors.
The NGS analysis reported here is for a single case, as suggested by this referee, we have modified this statement in the revised manuscript in the 'Methods' section.

Comment:

2. Figure 2A: Authors indicate yellow arrow showing palisading necrosis; is this the correct location?
Answer:
As suggested by the referee the corrections are made in this figure, and a new figure-2 and a new figure legend is added in the revised manuscript.

Comment:
3. Authors conclude they identified four known missense mutations, eight synonymous and seven

intronic, in this grade III ependymoma. How global these signature molecules in the context of grade III ependymoma? Can the authors add additional correlation analysis by analyzing TCGA or other bioinformatics-based data?

Answer:

As suggested by the reviewer we have searched various databases including The Cancer Genome Atlas (TCGA) www.tcga.org, and summarize our answer to the reviewer's comments below. A relevant section of this summary is included in the revised manuscript. The tumor type we described in this study is a rare tumor, and specifically, in many databases, it is not listed separately except in the 'Integrative onco-genomics' database (https://www.intogen.org).

In the integrative onco-genomics database (https://www.intogen.org/search?cancer) high-grade glioma and low-grade glioma, and GBM projects are listed. Genes mutated such as TP53, and PDGFRA are in high-grade glioma data from St. Jude children's research hospital (HGG_D_STJUDE), and IDH1, TP53, PIK3CA, EGFR, are most recurrently mutated cancer driver genes in GBM_TCGA dataset (https://www.intogen.org). Also, under 'ependymoma' only, two cohorts are found, with a total of 94 samples, 10,607 total mutations, and one driver gene is mutated in this.

In the ependymoma – DKFZ cohort, (EPD_PRY_DKFZ_2017), a total of 55 Samples, mutations with driver genes found are nil, total mutations found are 534, (Grobner et al., 2018). Ependymoma data from St. Jude children's research hospital cloud, 39 samples are found, with 1 driver gene mutated, mutations-10,073. By WGS, PIK3CA is detected as a mutational cancer driver in the ependymoma cohort. 2 out of 39 (5.13%) samples (3:179203765: T>A; AA, 345, 3:179221147: A>C, AA726), were found to have a mutation in this driver gene. (Parker et al., 2014).

We have analyzed the TCGA (https://www.intogen.org/search?cancer) release 2020-02-01, dataset. Tumor types such as medulloblastoma (636 samples), pilocytic astrocytoma (621 samples), GBM (571 samples), and LGG (565 samples) are included in this but not ependymoma. Glioblastoma was the first cancer studied by TCGA in a pilot study. In the TCGA projects top mutated cancer genes in IDH1, TP53, EGFR, PIK3CA, and PDGFRA. In the TCGA database the missense IDH1 mutation p.(R132H) affected cases are 90.07%, and VEP impact (Ensembl Variant Effect Predictor) is moderate for this, and SIFT impact is deleterious low confidence (score 0.01), and the PolyPhen impact is also possibly damaging (score 0.813). Poor prognostic markers included genetic changes in the EGFR and PI3-kinase mutations in this group. Among most driver mutations IDH1/2 and TP53 tumor grade remain a prognostic factor in diffuse gliomas (Draaisma et al., 2015). The variant we found in the present ependymoma case such as in TP53, HRAS, SMAD4, PIK3CA not in TCGA. However, in ClinVar database SMAD4 synonymous variant is reported (Accession: VCV000132693.2, Variation ID: 132693).

In cBioportal database (https://www.cbioportal.org) of whole-exome sequencing (WES) under diffuse glioma project for CNS/Brain tumors, only diffuse glioma, low-grade glioma, glioblastoma, medulloblastoma, and pilocytic astrocytoma and other brain tumors are classified, but ependymoma is not listed separately to apply the filter. As stated by the reviewer we can apply the search only globally under low-grade glioma (LGG) and glioblastoma (GBM World Health Organization grade IV)) projects, and for global mutation profiling not related to the variants, we described in our manuscript. On this portal under CNS/brain studies merged cohort of LGG and GBM; TCGA, (Ceccarelli et al., 2016) a total of 1102 samples are present in that 812 (72.4%) cases are with mutations.

In IDH1 gene somatic mutations found in 411 samples (50.6%). More than 90% of them are missense mutations. There is promising clinical data in patients with IDH1 codon R132-mutant glioma treated with the IDH1-targeted inhibitor Ivosidenib an FDA-approved drug in another indication. This mutated amino acid was identified as a recurrent hotspot (statistically significant) in a population-scale cohort of tumor samples of various cancer types (Chang et al., 2016).

Samples with TP53 mutations are 322 (39.7%), there are no FDA-approved or NCCN-compendium listed treatments specifically for patients with c.215C>G mutant diffuse glioma. Mutations in PIK3CA cases are 63 (7.8%). While Alpelisib in combination with Fulvestrant is FDA-approved for the treatment of patients with PIK3CA-mutant ER+/HER2- breast cancer, its clinical utility in patients with PIK3CA mutations in diffuse glioma is unknown. Mutations in EGFR cases are 87, (10.7%), laboratory data suggest that glioma cells with EGFR mutations may be sensitive to Lapatinib, an EGFR/HER2 tyrosine kinase inhibitor. While the EGFR tyrosine kinase inhibitor Afatinib is FDA-approved for the treatment of patients with EGFR G719-mutant non-small cell lung cancer, its clinical utility in diffuse glioma patients with EGFR mutations is unknown. PDGFRA mutations cases are 12 (1.5%), while Imatinib is NCCN-compendium listed for the treatment of patients with gastrointestinal stromal tumors (GISTs) harboring oncogenic PDGFRA alterations, its clinical utility in diffuse glioma patients with PDGFRA mutation is unknown. KDR case with mutations are 1%, there are no FDA-approved or NCCN-compendium listed treatments specifically for patients with KDR mutant diffuse glioma. FLT3 cases are 0.6%, while the multi-kinase inhibitor Midostaurin in combination with intensive chemotherapy is FDA-approved for the treatment of patients with FLT3 mutant acute myeloid leukemia (AML), its clinical utility in patients with FLT3 mutant diffuse glioma is unknown. RET and MET cases are 0.6%, APC cases are 0.2%, ERBB4 cases are 0.4%, no clinical data is available for these genes.

FGFR3 mutation cases are 0.2%, while there is promising clinical data in patients with urothelial cancer harboring functionally characterized hotspot FGFR3 mutations treated with pan-FGFR-targeted inhibitors such as AZD4547, BGJ398, Debio1347 and Erdafitinib, their clinical utility in patients with FGFR3 mutant diffuse glioma is unknown. None of the cases found to have SMARCB1, CSF1R, SMAD4, and HRAS, mutations. Whereas when we searched in a glioma cohort of 1004 samples (https://www.cbioportal.org/MSKCC, Jonsson et al., 2019) on this portal cases found to have SMARCB1, CSF1R, SMAD4, and HRAS mutations are 1.3%, 1.4%, 0.6%, and 0.2% respectively.

We have searched the database "Genomics of drug sensitivity in cancer" (cancerrxgene.org) to verify the studies targeting the signaling pathways of the four missense variants found in our studies. Compounds such as AGI-5198, GSK690693, Foretinib, and MIRA-1 shown to sensitize in GBM and LGG cell lines in vitro, targeting IDH1, PIK3CA, KDR, and TP53 pathways respectively (Iorio et al., 2016).

ICGC (https://dcc.icgc.org) data portal 2504 cases in 6 projects were reported; 3 projects from the US, 1 each from Canada, Germany, and China respectively. GBM-TCGA US-595 case, pediatric brain cancer-DE, -554 cases, LGG-TCGA, US, 514 cases were reported. In top 20 mutated cancer genes with high functional impact somatic mutations in 393 cases of LGG affected in IDH1, 24 cases of GBM affected in IDH1, 11 cases of pediatric brain cancer in IDH1, 229 cases of LGG in TP53, 105 cases of GBM in TP53, 42 cases of pediatric brain cancer in TP53, 10 cases of pediatric brain cancer in TP53. 13 cases of LGG in EGFR, 19 cases of GBM in EGFR. Other genes were not in Top 20 genes.

In the NCI's Genomic Data Commons (GDC) portal (https://portal.gdc.cancer.gov/) cases TCGA -GBM and TCGA -LGG are projects with 617, and 516 cases are reported, with mutations in 396, and 513 cases reported. IDH1 mutations were found in 394 out of 903 cases, cases were affected with mutations in TP53 are 233, 38 cases were affected in PIK3CA; EGFR, 95 cases, PDGFR 20 cases, in 2 projects.

IDH1 c.395G>A p.(R132H) mutation (rs121913500), are reported in GBM, astrocytoma, and oligodendrogliomas in Clin variant database, #VCV000156444. The frequency of this variant is highest (64.3%) in GBM WHO grade IV, compared with astrocytoma WHO grade II (7.14%), anaplastic oligodendroglioma WHO grade III (14.3%) and anaplastic ependymoma WHO grade III (14.3%) (Yusoff et al., 2016).   This variant also reported in AML as an adverse prognostic factor (Wagner et al., 2010). The NCI's genomic data commons (GDC) have reported 28 mutations in 102 affected cases with KDR mutations in all TCGA GBM projects. The expression KDR gene (vascular endothelial growth factor receptor 2 or VEGFR2) is increased in endothelial cells during tumor angiogenesis, and missense mutations cause constitutive activation of VEGFR2 in hemangioma. Patients with infantile capillary hemangioma are known to have constitutive activation of VEGFR2 signaling and carry a germline mutation (C482R) in the KDR gene (Jinnin, et al., 2008). TP53 c.215C>G, PIK3CA c.1173A>G, c.352+40A>G, EGFR c.2361G>A not reported in GDC.

SMAD4 mutation in c.1086T>C (rs1801250) reported in breast cancer (Tram et al., 2011); HRAS mutation in c.81T>C rs12628, reported in chronic myeloid leukemia (Mir et al., 2015), PIK3CA mutation in c.352+40A>G, rs3729674 in breast cancer (Arsenic et al., 2015) ; ERBB4 mutation in c.421+58A>G, rs839541 in brain tissue (Mothersill et al., 2012),

TP53 mutations in GBM mostly point mutations that lead to a gain of function (GOF) of the oncogenic variants of the p53 protein (Zhang et al., 2018). The TP53 variant rs1042522 we reported in the present case [(c.215C>G, p. (Pro72Arg)] was also reported in anaplastic astrocytoma grade-III (Pessoa et al., 2019), but not in ependymoma cases. In COSMIC database this variant is reported in several types of cancers. A mutation in Exon 5 of the TP53 gene was reported in one anaplastic ependymoma out of three cases (Tominaga et al., 1995). Whereas in our case the mutation was found in exon 4.

Targeted therapy is being studied for the treatment of childhood ependymoma and other brain tumors utilizing the genomic data. NCI supported Clinical Trials for Ependymomal brain tumors 4 clinical trials are listed (
https://www.cancer.gov/types/brain/patient/child-ependymoma-treatment-pdq). One study is enrolling the patients for drug targets (Carboplatin and Bevacizumab for Recurrent Ependymoma) that inhibit VEGF-promoted angiogenesis. Based on the interesting results observed in the reported small series of patients with recurrent ependymomas treated with bevacizumab, as well as on the evidence of VEGF-promoted angiogenesis in these tumors, we designed a phase II study to test the efficacy of bevacizumab in patients with recurrent ependymoma. Cabozantinib, a multi-kinase inhibitor of FLT3, MET, VEGFR2, and KIT, respectively, and clinical trials are undergoing for Non-Small Cell Lung Cancer, thyroid cancer, AML, and GBM treatment.

References:

Arsenic R, Treue D, Lehmann A, et al., Comparison of targeted next-generation sequencing and

Sanger sequencing for the detection of PIK3CA mutations in breast cancer. BMC Clin Pathol. 2015; 15:20. doi: 10.1186/s12907-015-0020-6. eCollection 2015.

Chang MT, Asthana S, Gao SP, et al., Identifying Recurrent Mutations in Cancer Reveals Widespread Lineage Diversity and Mutational Specificity. Nat Biotechnol. 2016; 34: 155-163. doi: 10.1038/nbt.3391.

Ceccarelli M, Barthel FP, Malta TM, et al., TCGA Research Network; Noushmehr H, Iavarone A, Verhaak RGW. Molecular Profiling Reveals Biologically Discrete Subsets and Pathways of Progression in Diffuse Glioma (Ceccarelli et al., 2016).

Draaisma K, Wijnenga MMJ, Weenink B, et al., PI3 kinase mutations and mutational load as poor prognostic markers in diffuse glioma patients. Acta Neuropathologica Communications. 2015; 3:88 DOI 10.1186/s40478-015-0265-4.

Grobner SN, Worst BC, Weischenfeldt J, et al., ICGC PedBrain-Seq Project; ICGC MMML-Seq Project. The Landscape of Genomic Alterations Across Childhood Cancers. Nature. 2018; 555 :321-327. doi: 10.1038/nature25480.

Iorio F, Knijnenburg TA, Vis DJ, et al., A landscape of pharmacogenomic interactions in cancer. Cell. 2016; 166: 740 – 754. doi: 10.1016/j.cell.2016.06.017.

Jinnin, M, et al., Suppressed NFAT-dependent VEGFR1 expression and constitutive VEGFR2 signaling in infantile hemangioma. Nature Med. 14: 1236-1246, 2008.

Jonsson P, Lin AL, Young RJ, et al., Genomic Correlates of Disease Progression and Treatment Response in Prospectively Characterized Gliomas. Clin Cancer Res. 2019; 25: 5537-5547. doi: 10.1158/1078-0432.CCR-19-0032.

Mir R, Ah I, Javid J, et al., Polymorphism T81C in H-RAS Oncogene Is Associated with Disease Progression in Imatinib (TKI) Treated Chronic Myeloid Leukemia Patients. World J Oncol. 2015; 6: 321-328. DOI: 10.14740/wjon912e.

Mothersill O, Kelly S, Rose EJ, Donohoe G. The effects of psychosis risk variants on brain connectivity: a review. Front Psychiatry. 2012; 3:18. doi: 10.3389/fpsyt.2012.00018.

Parker M, Mohankumar KM, Punchihewa C, et al., C11orf95–RELA fusions drive oncogenic NF-κB signalling in ependymoma. Nature. 2014; 506: 451–455.

Pessoa IA, Amorim CK, Ferreira WAS, et al., Detection and Correlation of Single and Concomitant TP53, PTEN, and CDKN2A Alterations in Gliomas. Int J Mol Sci. 2019; 20 (11). pii: E2658. doi: 10.3390/ijms20112658.

Tominaga T, Kayama T, Kumabe T, et al., Anaplastic ependymomas: clinical features and tumour suppressor gene p53 analysis. Acta Neurochir (Wien). 1995; 135(3-4):163-70. https://doi.org/10.1007/BF02187763.

Tram E, Ibrahim-Zada I, Briollais L, et al., Identification of germline alterations of the mad homology 2 domain of SMAD3 and SMAD4 from the Ontario site of the breast cancer family registry (CFR). Breast Cancer Res. 2011 ;13(4): R77. doi: 10.1186/bcr2926.

Wagner K, Damm F, Göhring G, et al., Impact of IDH1 R132 Mutations and an IDH1 Single Nucleotide Polymorphism in Cytogenetically Normal Acute Myeloid Leukemia: SNP rs11554137 Is an Adverse Prognostic Factor. J Clin Oncol. 2010; 28: 2356-2364. doi: 10.1200/JCO.2009.27.6899.

Yusoff AM, Zulfakhar FN, Sul'ain MD, et al., Association of The IDH1 C.395G>A (R132H) Mutation with Histological Type in Malay Brain Tumors. Asian Pac J Cancer Prev. 2016 ;17: 5195-5201. doi:10.22034/APJCP.2016.17.12.5195.

Zhang Y, Dube C, Gibert M Jr, et al., The p53 Pathway in Glioblastoma. Cancers (Basel). 2018 Sep 1;10(9). pii: E297. doi: 10.3390/cancers10090297.

Comment:
4. Authors indicate FLT3 (c.1776T>C, synonymous) is novel, which is interesting; is this mutation reported in other cancer than ependymoma? What is the clinical and functional significance of this mutation in ependymoma progression?

Answer:
A relevant section is added to the revised manuscript regarding this comment. This mutation is not reported in the merged cohort of LGG and GBM-TCGA project (Ceccarelli et al., 2016). This driver gene FLT3 down-regulation is related to favorable clinical outcome in glioma patients (Liang et al., 2017). Interestingly, several pathogenic mutations were reported at Val592 coding positions c.1774 and c.1775 in the COSMIC database but all in acute myeloid leukemia (AML). However, the FLT3 synonymous mutation found in our ependymoma case (c.1776T>C) is within the juxta-membrane domain in exon 14, which codes the same amino acid valine p. (Val592Val), hence we don't anticipate having any functional and clinical impact of this mutation. This variant is not reported in the COSMIC database or dbSNP also. The most common form of FLT3 mutation is in the internal tandem duplication (ITD) region of the juxta-membrane domain (AA 572-609), which occurs in 15–35% of patients with AML (Staudt et al., 2018). The presence of either a FLT3 ITD or TKD mutation may be associated with a response to the tyrosine kinase inhibitor, Midostaurin (Stone et al., 2017). FLT3 activating mutations were predominant in AML, and types of leukemias and lymphomas also (Metzeler et al., 2016; The AACR Project GENIE Consortium). In the database of Genomics of Drug Sensitivity in Cancer, https://www.cancerrxgene.org/compound, mutations in FLT3 are associated with altered sensitivity to several drugs tested in vitro, also several clinical trials are ongoing using these compounds (Daver et al., 2019).

References:

Staudt D, Murray H, McLachlan T, et al., Targeting Oncogenic Signaling in Mutant FLT3 Acute Myeloid Leukemia: The Path to Least Resistance. Int. J. Mol. Sci. 2018, 19, 3198;

doi:10.3390/ijms19103198

Liang, A., Zhou, B. and Sun, W. Integrated genomic characterization of cancer genes in glioma. Cancer Cell Int 2017; 17: 90. https://doi.org/10.1186/s12935-017-0458-y.

Daver N, Schlenk RF, Russell NH and Levis MJ. Molecular targets for therapy Targeting FLT3 mutations in AML: review of current knowledge and evidence. Leukemia. 2019; 33: 299–312. doi: 10.1038/s41375-018-0357-9.

Metzeler KH, Herold T, Rothenberg-Thurley M, et al., AMLCG Study Group. Spectrum and prognostic relevance of driver gene mutations in acute myeloid leukemia. Blood. 2016; 128: 686-698. doi: 10.1182/blood-2016-01-693879.

Stone RM, Mandrekar SJ, Sanford BL, et al., Midostaurin Plus Chemotherapy for Acute Myeloid Leukemia with a FLT3 Mutation. N Engl J Med. 2017; 377: 454-464. doi: 10.1056/NEJMoa1614359.

The AACR Project GENIE Consortium. AACR Project GENIE: powering precision medicine through an international consortium. *Cancer Discovery*. 2017; 7: 818-831. DOI: 10.1158/2159-8290.CD-17-0151.

Competing Interests: Nil.

The benefits of publishing with F1000Research:

- Your article is published within days, with no editorial bias

- You can publish traditional articles, null/negative results, case reports, data notes and more

- The peer review process is transparent and collaborative

- Your article is indexed in PubMed after passing peer review

- Dedicated customer support at every stage

For pre-submission enquiries, contact research@f1000.com

F1000Research